Russian Chemical Reviews **77** (3) 233 – 257 (2008) © 2008 Russian Academy of Sciences and Turpion Ltd

DOI 10.1070/RC2008v077n03ABEH003751

Synthesis and properties of silver nanoparticles: advances and prospects

Yu A Krutyakov, A A Kudrinskiy, A Yu Olenin, G V Lisichkin

Contents

I.	Introduction	233
II.	Conventional syntheses of silver nanoparticles	234
III.	Unconventional syntheses of silver nanoparticles	240
IV.	Shape-controlled synthesis of silver nanoparticles	243
V.	Optical properties of silver nanoparticles	246
VI.	Antibacterial properties of nanosilver	251
VII.	Conclusion	253

Abstract. Conventional and novel syntheses of silver nanoparticles are considered, their advantages and shortcomings are analysed. Attention is focused on the shape-controlled methods of preparation of nanosized particles. The unique optical and antibacterial properties of nanosilver and related applications are discussed. The bibliography includes 285 references.

I. Introduction

Extraordinary optical properties of silver nanoparticles (NP) were used (of course, only unconsciously) by glass founders as far back as in the times of the Roman Empire. This is evidenced by the so-called Lycurgus cup (IV century AD) now exposed in the British Museum. A detailed study of the composition of its bronze-mounted insets of stained glass, carried out in the late 20th century, revealed the presence of metal NP (with the average diameter of 40 nm) that consisted of a silver (70%) and gold (30%) alloy.[1] This explained a remarkable feature of this bowl to change its colour from red in transmitted light to greyish green in reflected light. In the preparation of this glass, nanosilver was formed *in situ*. A similar example of the use of this metal is lemon-yellow glass in old European cathedrals.

Before the 1980s, the scientific and practical interest in silver NP was exclusively caused by the possibility of their use as highly dispersed supports for enhancing the signals from organic molecules in the Raman spectroscopy.[2,3] Furthermore, antibacterial agents (such as collargol) based on colloidal silver proved to be highly efficient in medicine. Fundamental studies carried out in the 1980s and1990s showed that silver NP exhibit a rare combination of valuable properties, namely, unique optical properties associated with the surface plasmon resonance (SPR), well-developed surfaces, catalytic activity, high electrical double layer capacitance, *etc*.[4] This is why they serve as a material in the development of new-generation electronic, optical and sensor devices. In the past twenty years, the trend towards miniaturisation and the necessity of modernisation of technological processes led to the substantial increase in the number of scientific publications devoted to the synthesis and properties of silver NP; at present, their synthesis is among the most actively developing trends of colloid chemistry.

Notwithstanding the fact that as compared with gold particles, silver NP have excellent optical properties and display a unique ability for amplifying signals in fluorescence and Raman spectroscopies,[5–7] the former particles find wider scientific and practical application due to their chemical inertness and simple synthesis.[8] In contrast, silver NP non-stabilised in a proper way undergo fast oxidation and easily aggregate in solutions, which complicates their use in the development of sensors and optical instruments. Silver is more reactive than gold; hence, first of all, the methods for the synthesis and effective stabilisation of NP with narrow size distributions must be elaborated. From our viewpoint, the well-known problem of coupling the synthesis of NP with the preparation of an appropriate modifier of their surface is by no means an insurmountable obstacle in the production of stable nanomaterials and their further use.[9]

In this review, the majority of known (conventional and unconventional) methods of production of silver NP are considered, their advantages and drawbacks are analysed. Moreover, attention is focused on the shape-controlledsynthesis. Unique optical and antibacterial properties typical of silver NP are also discussed.

Yu A Krutyakov, A A Kudrinskiy, A Yu Olenin, G V Lisichkin
Department of Chemistry, M V Lomonosov Moscow State University, Leninskie Gory, 119991 Moscow, Russian Federation,
Fax (7-495) 939 46 38, tel. (7-495) 939 35 49,
e-mail: yurii@petrol.chem.msu.ru (Yu A Krutyakov),
kudrinskii@petrol.chem.msu.ru (A A Kudrinskiy),
olan@petrol.chem.msu.ru (A Yu Olenin), tel. (7-495) 939 46 38,
e-mail: lisich@petrol.chem.msu.ru (G V Lisichkin)

Received 5 October 2007
Uspekhi Khimii **77** (3) 242 – 269 (2008); translated by T Ya Safonova

II. Conventional syntheses of silver nanoparticles

1. Citrate synthesis (the Turkevich method)

In 1951, Turkevich *et al.*[10] described a synthesis of hydrophilic gold NP by the reduction of chloroauric acid with sodium citrate in an aqueous solution on boiling. According to the data from transmission electron microscopy (TEM), the synthesised NP were spherical, had a narrow size distribution and the average diameter of 20 ± 1.5 nm. Later, the Turkevich method was used [3] in the preparation of silver NP. However, whereas Turkevich managed to obtain spherical gold NP with a narrow size distribution, for silver, the diameter of synthesised different-shaped aggregates varied in the range of 60–200 nm. Despite its considerable drawbacks, the citrate method was widely used for the synthesis of silver NP.[11–13] A distinguishing feature of the Turkevich method is that citrate ions simultaneously act as a reducing agent and a stabiliser. This complicates the selection of their optimal concentration, because its variations simultaneously affect the reduction rate and the nucleation and growth of particles. Moreover, the oxidation products of citrate anions (acetonedicarboxylic and itaconic acids) can adsorb on the NP surface thus affecting their further growth. Apparently, to elucidate the stabilising role of citrate anions, one has to reduce a metal salt under conditions unfavourable for the reduction of metal ions with citrate (*e.g.*, at room temperature). Henglein *et al.* accomplished this process.[14] The reducing agent represented hydroxyalkyl radicals formed *in situ* in the course of γ-radiolysis (^{60}Co, 9.3×10^4 rad h^{-1}) of a solution of $AgClO_4$ in aqueous isopropyl alcohol containing N_2O

$$e_{aq}^- + N_2O + H_2O \longrightarrow N_2 + HO^- + HO^\bullet,$$

$$HO^\bullet\,(H^\bullet) + Me_2CHOH \longrightarrow H_2O\,(H_2) + Me_2C^\bullet OH,$$

$$Ag^+ + Me_2C^\bullet OH \longrightarrow Ag + Me_2CO + H^+. \qquad (1)$$

Solvated electrons and H$^\bullet$ and HO$^\bullet$ radicals did not react with the citrate ion. Hence, the latter was merely a 'spectator' in the reduction process but played an important role in stabilisation of particles formed. At low and high citrate concentrations (5×10^{-5} and 1.5×10^{-3} mol litre^{-1}, respectively), coarse and defective silver aggregates 15–30 nm in diameter were formed, whereas at intermediate concentrations of the stabilising agent [in the range of $(1-5) \times 10^{-4}$ mol litre^{-1}], spherical NP with a sufficiently narrow size distribution (8–11 nm in diameter) were obtained. The mentioned facts made it possible to assume that different NP growth mechanisms are realised under the described conditions and that citrate plays the key role in them.

Due to a sufficiently high standard reduction potential of the Ag^+/Ag^0 pair ($E^\circ = 0.799$ V), reaction (1) is relatively slow; however, its rate is sufficient to successfully compete with the reactions of scavenging of hydroxyalkyl radicals in solution at a given radiation dose.[15] Two alternative mechanism of particle growth were proposed (Fig. 1).[14] In both cases, the initial stage of reduction afforded clusters Ag_2^+, Ag_4^+, Ag_9^+, *etc.* (generally, Ag_x) the structure of which was found by pulse radiolysis [16] and confirmed later by mass spectral studies;[17] particularly, it was shown that the formation of Ag_3 and Ag_3^+ clusters plays the key role in the growth of triangular silver NP. The nascent Ag_x clusters reacted with citrate (cit), which was followed by their aggregation into coarser particles:

$$Ag_{x(cit)} + Ag_{x(cit)} \longrightarrow Ag_{2x(cit)}, \textit{ etc.}$$

Upon reaching the critical size (50–100 atoms or 1–1.5 nm), the clusters virtually ceased to grow by the condensation mechanism and, at low citrate concentrations,

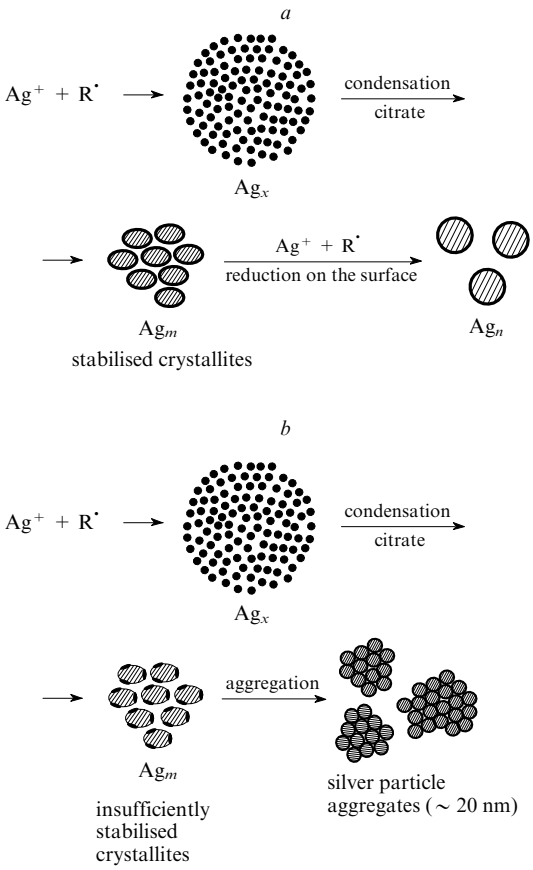


Figure 1. Growth mechanisms of silver NP stabilised by citrate anions (see text).[14]
Ag_x are silver clusters (<1 nm), Ag_m are primary citrate-stabilised particles (~1 nm), Ag_n are final particles, R$^\bullet$ are reducing radicals.
Citrate concentration was 5×10^{-5} or 1.5×10^{-3} mol litre^{-1} (*a*) and 5×10^{-4} mol litre^{-1} (*b*).

its stabilising action was insufficient to prevent the aggregation of clusters, which led to NP of larger diameters. At higher citrate concentrations, the solution ionic strength reached large magnitudes sufficient for destabilisation of the citrate layer, which also resulted in coagulation. Attention should be drawn to the mechanism of NP growth at intermediate citrate concentrations, namely, $(1-5) \times 10^{-4}$ mol litre^{-1}, where the stabilisation of clusters was more reliable and virtually no coagulation was observed (see Fig. 1 *a*). In this case, particles continued to grow but by a different mechanism [18–21] according to which the growth occurred as a result of reduction of silver ions on the cluster surface.

$$Ag_{mx(cit)} + n\,Me_2C^\bullet OH \longrightarrow Ag_{mx(cit)}^{n-} + n\,Me_2CO + n\,H^+,$$

$$Ag_{mx(cit)}^{n-} + Ag^+ \longrightarrow Ag_{(mx+1)(cit)}^{(n-1)-}.$$

Hence, after the cluster nucleation, its further growth proceeded gradually. Silver NP formed by this mechanism were unsusceptible to aggregation, spherical and had narrow size distribution.

The Turkevich process was also studied in more detail.[22] Based on spectral data, it was confirmed that the degree of reduction of silver ions depends on the citrate concentration and also on the time of solution boiling. Thus the maximum degree of reduction was reached in 40 min for a molar ratio [Ag] : [cit] = 1 : 1 [$c(AgNO_3) = 1$ mmol litre^{-1}] and in 15 min

for [Ag] : [cit] = 1 : 5. Calculations of the effective constant of binding of the citrate anion to the silver NP surface involved carrying out spectral studies of the interaction of citrate anions with silver NP adsorbed on silica gel colloid particles. The presence of two peaks in the absorption spectrum, namely, a peak at $\lambda = 380$ nm corresponding to NP with the 'bare' surface and a peak at $\lambda = 410$ nm corresponding to nanoparticles with chemisorbed citrate ions, and of an isobestic point made it possible to assume the existence of an equilibrium

$$SiO_2-Ag + cit \rightleftharpoons (SiO_2-Ag-cit)$$

with the effective constant $K = 220$ litre mol^{-1}. The pulse radiolysis methods used in the studies of mechanisms of silver NP growth confirmed the earlier results on this subject.

2. Borohydride method

At present, reduction of silver salts with sodium borohydride is the most widely used method of synthesis of silver NP in both homogeneous and heterogeneous systems.[23] This is explained by the relatively high reactivity of borohydride (as compared with citrate and carbohydrates), its handiness (as compared with gaseous hydrogen and physical methods) and not too high toxicity (as opposed to hydrazine and hydroxylamine). One of the first publications [2] on the preparation of silver NP by the borohydride method described the reduction of an $AgNO_3$ solution cooled to 0 °C with a sixfold excess of $NaBH_4$ solution on active stirring. The diameter of formed particles fell in the range of 1–10 nm and a band with the maximum at $\lambda = 400$ nm was present in the absorption spectrum. Such a colloid solution was used later for amplifying the Raman signal of pyridine preliminarily chemisorbed on the surface of silver NP. The synthesis of silver NP stabilised by poly(vinyl alcohol) (PVA) was reported,[3] which involved the reduction of $AgNO_3$ in an aqueous solution with a 1.2-fold excess of $NaBH_4$ in the presence of PVA.

The mechanisms of NP growth remained unclear for a long time and it was assumed that all the processes obeyed to one or another extent to the LaMer–Dinegar model.[24] This states that the number of colloid particles in solution is established during a short period of nucleation and then remains unchanged. The further growth of particles occurs by the reduction of ions on the surface of formed clusters. In the late 1980s, it was shown [25, 26] that the cluster aggregation step might play the key role in the formation of colloid particles. The formation of spherical NP in the reduction of aqueous silver perchlorate solutions with sodium borohydride was studied.[27] The reduction involved several stages each corresponding to a certain solution colour. In the first stage (for ~0.5–1 s), the solution was dark muddy-green (with a characteristic absorption band at $\lambda = 220$ nm), on going to the second stage (duration ~45 min) the colour changed to light yellow ($\lambda \approx 400$ nm) and, in the final stage, the solution again darkened ($\lambda \approx 500-800$ nm). The experiments involved varying both the molar ratio $[NaBH_4] : [AgClO_4]$ (from 2 to 12) and the temperature (from 5 to 25 °C). Based on spectral data, the characteristic band at $\lambda = 220$ nm, which was observed in all experiments in the initial stage of the process, was attributed to the shift of the absorption band maximum ($\lambda = 190$ nm) of the borohydride anions adsorbed on silver clusters (measuring 1–2 nm) with a large specific surface area. However, the latter structures were not identified. In the second stage, the absorbance sharply increased at a wavelength of 390 nm and decreased at $\lambda = 220$ nm. This was explained by the increase in the size of silver NP caused by association of clusters into coarser aggregates (7–9 nm). To verify the NP growth mechanism, the loss of silver ions in the course of synthesis was studied. Samples taken in different moments of growth were subjected to elemental analysis for the content of Ag^+ ions; the amount of Ag^+ ions proved to be the same in all the cases. Thus, all silver was reduced in the first seconds of the process, which made impossible the further growth of NP by reduction of ions on its surface. In the final stage, the aggregation of particles occurred due to the decomposition of borohydride, which simultaneously acts as the reducing agent and the NP stabiliser. The aggregative stability of silver NP dispersions was studied at different temperatures and $NaBH_4$ concentrations,[27] which also involved measuring the electrochemical potential of solution (with respect to the standard calomel electrode). Colloid solutions proved to be stable at potentials below −200 mV; at higher potentials, especially at low temperature (5 °C), spontaneous coagulation of NP was observed. Several other publications were devoted to aggregative stability of silver NP dispersions formed in the reduction with sodium borohydride.[28, 29]

Evidently, the preparation of silver NP with the preset properties and long-term stability requires a stabiliser to be introduced during their synthesis. In Russia, several fundamental studies of the coordination chemistry and stabilisation of metal clusters were carried out by Gubin. Certain aspects of the coordination interaction of NP with stabiliser molecules were comprehensively surveyed in detail in a review.[30]

One of a few studies known to date on the synthesis of stable silver NP with positively charged surfaces involved the use of bis(11-trimethylammonioundecanoylaminoethyl) disulfide dibromide as the stabiliser [31]

$$[Me_3\overset{+}{N}(CH_2)_{10}C(O)NH(CH_2)_2S_2(CH_2)_2NHC(O)(CH_2)_{10}\overset{+}{N}Me_3](Br^-)_2 .$$

Reduction of disulfide with sodium borohydride in the aqueous phase afforded thiol that exhibits enhanced reactivity with respect to the surface of the metal NP. The prepared NP were stable in solutions with pH from 5 to 9 but completely aggregated at pH 1 and 14. The synthesis of stable silver NP stabilised with the peptide Cys-Ala-Leu-Asp-Asp and mercaptoalkylated polyethylene glycol (PEG-R), namely, $HS(CH_2)_{11}.(OCH_2CH_2)_4R$ (R = OH, NH_2), was described.[32]

In the first step, citrate-stabilised NP were synthesised by a method described in Ref. 3; then, they were modified by a ligand exchange reaction in a buffer solution. Peptide-stabilised samples demonstrated high stability in 1 M NaCl in the pH range from 4 to 12. Particles modified with PEG-OH and PEG-NH_2 exhibited high stability in 2 M NaCl in the pH range from 1 to 14. The synthesis of moderately polydispersed water-soluble silver NP (2.5–5 nm) stabilised by 2-mercaptoethanesulfonic acid was reported.[33] Obviously, the stability of thus prepared colloids was due to the electrostatic repulsion between NP with negatively charged surfaces. However, the electric double layer of particles was destabilised and they completely coagulated even in 0.1 M NaCl and 0.01 M HCl. Silver NP with the average diameter of 8 nm, stabilised by sodium 3-mercaptopropanesulfonate, were synthesised in the reduction of an AgI hydrosol.[34, 35] Their properties did not differ from those described in the previous study. A synthesis of silver NP with the average diameter of 17 nm also stabilised by 3-mercaptopropanesulfonic acid was reported.[36]

A substantial drawback of most syntheses conducted in aqueous media was the impossibility to reach high concentrations of silver NP in final solutions (only

$< 10^{-4}$ mol litre^{-1}), which is associated with their aggregative instability. In this respect, attention should be drawn to an approach [37] that represents the reduction of concentrated silver nitrate solutions with sodium borohydride in the presence of a synthetic inorganic material, Laponite. The stabilisation mechanism consisted of the adsorption of clusters on the Laponite surface, which made impossible their aggregation. The only way to increase the particle size was their growth by the reduction of silver ions on the surface of an adsorbed cluster. This allowed sols with the high silver contents (7.35×10^{-2} mol litre^{-1}) and the average particle size of 7–10 nm to be prepared.

3. Synthesis in two-phase water–organic systems

In 1851, at the Royal Society Meeting, Faraday presented a hydrosol of gold NP, which was synthesised in a two-phase system by the reduction of aqueous $AuCl_3$ with white phosphorus dissolved in carbon disulfide on vigorous stirring. Later, this method was reproduced in many studies. Turkevich *et al.*[10] synthesised spherical gold NP with the diameter of 5 nm by the Faraday method in which diethyl ether was substituted for carbon disulfide. Thus, they demonstrated the advantage of two-phase systems over single-phase, which lies in the possibility of exercising a more flexible and effective control over the average size of synthesised particles.

One of the most important milestones in the development of two-phase water–organic synthesis of noble metal nanoparticles was a study [38] which contained the first description of a method (now known as the Brust–Schiffrin method) for synthesising hydrophobic gold nanoclusters (1–3 nm) stabilised by a self-assembled monolayer of an alkanethiol, carried out in a two-phase water–organic system. Virtually all so-far known methods of preparation of silver NP in two-phase water–organic systems are based on the Brust–Schiffrin method and differ only in details of the process. The idea of this synthesis lies in the preparation of NP from reactants spatially separated into two immiscible phases. The reaction rate between a metal precursor and a reducing agent is limited by the interface area between two liquids and also by the intensity of the reactant transfer from aqueous to organic medium by a quaternary alkylammonium salt. Stabilisation and hydrophobisation of clusters formed at the interface occurs as a result of their coverage with an alkanethiol monolayer that resides in the non-polar medium. Brust and Schiffrin used toluene as the non-polar medium and tetra-n-octylammonium bromide as the phase transfer agent

$$H^+(aq) + AuCl_4^-(aq) + N(n\text{-}C_8H_{17})_4Br(org) \longrightarrow$$

$$\longrightarrow N(n\text{-}C_8H_{17})_4AuCl_4(org) + H^+(aq) + Br^-(aq),$$

$$m(AuCl_4)N(n\text{-}C_8H_{17})_4(org) + n(n\text{-}C_{12}H_{25})SH(org) + 3me^- \longrightarrow$$

$$\longrightarrow 3mCl^-(aq) + (Au_m)(n\text{-}C_{12}H_{25}SH)_n(org) + mN(n\text{-}C_8H_{17})_4Cl(org).$$

With the substitution of silver for gold, the reduction process looses its illusive simplicity and clarity. Indeed, to be extracted into a non-polar medium, an ion of a metal precursor should be electrostatically bound to a hydrophobic carrier and whereas for gold this merely involved the formation of an ion pair $N(n\text{-}C_8H_{17})_4^+[AuCl_4]^-$, for a positively charged Ag^+ ion such interaction becomes impossible. Nonetheless, the Brust–Schiffrin process was widely applied in the preparation of organosols of metallic silver.[39–41]

A distinguishing feature of a method that employs $AgNO_3$ as the precursor lies in the fact that particles of silver bromide sol formed in ordinary ion exchange between the phase transfer agent and metal salt molecules fail to precipitate due to their small size. Moreover, AgBr particles acquire a negative charge as a result of adsorption of bromide ions; this make possible the further transport of particles to the non-polar medium by tetra-n-octylammonium bromide cations (virtually the only compound employed as the phase transfer agent in two-phase water–organic syntheses of nanoparticles). In contrast to homogeneous systems and micellar solutions for which the mechanisms and the kinetics of silver NP growth were elucidated with high degree of certainty, only a few studies dealt with the formation of the metal NP in two-phase water–organic systems. It is only known from spectral data that coarse aggregates are formed in the organic phase in the very beginning of reduction to disintegrate later to smaller particles.[40] A considerable drawback of this method is the difficulty of exerting simultaneous control over the growth of AgBr and metallic silver particles. Indeed, presumably, the final size of silver NP depends on the size of bromide particles and the coefficient of bromide distribution between the phases.

A synthesis of silver NP with separated steps of preparation of a hydrosol of negatively charged AgBr particles and their reduction to the metal was proposed.[42] This approach became possible due to the development of special methods for the synthesis of silver halide colloids.[43] As was noted,[42] a toluene solution containing AgBr particles and prepared by the extraction of silver bromide particles from an aqueous medium (milky white) was entirely transparent, despite the very different refraction indices of toluene and silver bromide. This suggests that the size of AgBr particles increases according to the dissolution–deposition mechanism. During the reduction process (4-bromobenzenethiol as the stabiliser), the spectrum revealed an absorption peak with $\lambda = 516$ nm that decayed in time. Taking into account the results obtained by Mulvaney,[44] the absorption at this wavelength was attributed [42] to particles that consisted of a metallic silver core and a shell of a subnanometer silver bromide layer. This peak disappeared by the end of the process, which points to the complete reduction of silver bromide and the formation of the metal NP (3.1–5.9 nm).

A substantial drawback of the Brust–Schiffrin method is the use of a large number of chemicals, particularly, the phase transfer agent that contaminates the surface of formed NP thus preventing their further use. In connection with this, a synthesis of silver NP from a silver nitrate complex with *N*-hexadecylethylenediamine (hex-en), $Ag(hex\text{-}en)_2NO_3 \cdot H_2O$, deserves mention.[45] The hydrophobic moiety of the hex-en molecule is responsible for the dissolution of the silver complex in the non-polar medium. The presence of two nitrogen atoms with lone pairs in the structure makes possible the ligand coordination to the surface and the stabilisation of silver NP. Thus, this method has the following two advantages: first, the possibility of using the ligand involved in the silver complex as a stabiliser of particles due to its pronounced chelation effect and, second, the absence of phase transfer agents that can contaminate the final product.[46] Moreover, varying the complex concentration allows one to prepare NP with different average diameters (from 7 to 14 nm). n-Butylamine served as the solvent for silver nitrate and n-dodecanoic acid was used as the stabiliser of monodispersed silver NP.[47]

The preparation of NP in an aqueous medium followed by their extraction into a non-polar medium containing a stabiliser may serve as an alternative to the two-phase synthesis of hydrophobic NP, where the phase transfer agent may act as the stabiliser.[48] A method was proposed [49] for hydrophobisation

of silver NP primarily stabilised by mercaptosuccinic acid, which involved their quantitative transfer into the organic medium by cetyltrimethylammonium bromide (CTMA) due to the electrostatic interaction of its molecules with carboxylate anions on the NP surface. Excessive CTMA was removed by its treatment with an aqueous solution of β-cyclodextrin.

A new two-step extraction method was elaborated [9] aimed at the preparation of hydrophilic silver NP stabilised by hydrophilic low-molecular organic ligands. The scheme of synthesis included preliminary preparation of hydrophobic silver NP stabilised by salts of quaternary ammonium bases in a two-phase water – organic medium, followed by the NP extraction from the organic medium to an aqueous solution containing a hydrophilic stabiliser. In the formation of NP, quaternary ammonium salts acted as phase transfer agents and hydrophobic stabilisers of NP. Their use made it possible to control the NP growth during the reduction and subsequent transition to the organic phase. The interaction of ammonium salts with the NP surface is due to electrostatic forces; hence, the further ligand exchange on the surface is possible. When a hydrophilic stabiliser is extracted to an aqueous solution, this exchange is accompanied by the NP polarity reversal. Thus, the shown scheme allows one to prepare hydrophilic NP using the methods developed for the synthesis of hydrophobic NP.

4. Organic reducing agents

The well-known Tollens reaction conventionally used for the chemical deposition of thin silver coatings may also be applied in the production of silver NP [50–53]

$$[Ag(NH_3)_2]^+(aq) + RCHO(aq) \longrightarrow Ag(s) + RCOOH(aq),$$

where RCHO is an aldehyde or a carbohydrate. Ready-made silver-plating solutions that contained a silver ammonium complex and formaldehyde were used.[50] Results obtained in this study on the NP nucleation and growth are consistent with the results reported earlier.[28,29] The average NP diameter was shown to depend on the temperature of the process ($\sim$20, $\sim$30 and $\sim$40 nm for 27, 30 and 35 °C, respectively). The obtained solutions exhibited long-term aggregative stability. It was shown [51] that fructose is more suitable than glucose as a reducing agent in the production of silver NP with small sizes (10 nm). It was assumed that the higher reductive ability of glucose favours the primary formation of a large number of small clusters with a low coagulation barrier; their further irreversible aggregation was responsible for the presence of coarser agglomerates. On the other hand, the reduction with fructose initially produced a smaller number of sufficiently coarse particles with a high coagulation barrier; their further growth was consistent with the aforementioned LaMer – Dinegar model.[24]

The size of silver NP was found to depend on the ammonia concentration and the pH of the medium during the reduction.[53] The following four carbohydrates were used as the reducing agents: glucose, lactose, maltose and galactose. The optimum conditions for the synthesis of relatively small particles with moderate degrees of polydispersion included the low bulk concentration of ammonia and the use of maltose as the reducing agent. When the NH_3 concentration was changed from 0.005 to 0.2 mol litre^{-1}, the average NP diameter increased from 25 to 260 nm. It is known that to conduct the Tollens reaction, a sufficiently high solution pH should be maintained, which is usually accomplished by adding inorganic bases. Alkali metal ions contaminate the surface of the metal NP, which is unacceptable from the viewpoint of their further use in various electronic devices. As an alternative to alkali metal hydroxides, organic bases (pyridine and triethylamine) were proposed.[54] The reduction was carried out with formaldehyde in an aqueous medium in the presence of poly(*N*-vinyl-2-pyrrolidone) (PVP) as the stabiliser. The use of sufficiently strongly basic triethylamine resulted in the formation of coarser NP (20 – 30 nm), the use of pyridine led to finer NP (10 – 20 nm).

An unusual version of the Tollens reaction employed [55] in the preparation of nanosilver involved the use of an extract of *Aloe vera* leaves. According to IR spectroscopic data, the carbonyl-containing low-molecular compounds in the *Aloe vera* extract were responsible for the reduction of an ammoniacal solution of $[Ag(NH_3)_2]OH$. Note that in contrast to the aforementioned studies based on the conventional Tollens reaction, this method made it possible to obtain spherical silver NP of small sizes (15.2 ± 4.2 nm). Earlier, the same authors reported [56] on the use of an extract of geranium leaves in the synthesis of silver NP.

The other organic solvents used in the production of monodispersed silver NP included ethanol,[57] ethylene glycol,[58,59] tri-n-octylphosphine,[60] *N*,*N*-dimethylformamide,[61] systems tri-n-octylphosphine – tri-n-octylphosphine oxide and oleic acid — octadecenylamine, [62–64] *etc*.

5. Synthesis in inverse micelles

A micellar system may be considered as a set of nanoscale chemical 'reactors' formed by surfactant molecules. The synthesis of silver NP consists of mixing two inverse emulsions (of the 'water-in-oil' type) of which one contains a silver salt dissolved in solubilised water and the other contains a reducing agent.

The virtue of the microemulsion method is the possibility of easy control over the diameter of formed NP by varying the molar ratio (W_0) water : surfactant (and, as a consequence, the diameter of the micelle water core) in the reaction medium. Active development of the inverse emulsion method started nearly 25 years ago.[65–73] A very clear mechanism proposed [69,70] for the NP formation in inverse micelles involves the following four main stages: (i) coalescence of water cores of colliding micelles (k_{ex}); (ii) a chemical reaction between components of solubilised solutions (k_{chem}); (iii) nucleation (k_n); (iv) intramicellar growth (k_g) of NP nuclei according to the Smoluchowski coagulation model (Fig. 2).

The process of NP formation and their size depended on the molar ratio water : hydrocarbon, the concentrations of metal ions and the reducing agent in micelles and, what is very important, the type of non-polar solvent used as the dispersion medium. The quantitative description of the mechanism of NP formation can be found in the original publications mentioned above.

Among the first syntheses of silver NP performed in inverse micelles were the processes carried out [74,75] by chemical or photochemical reduction of silver nitrate in the presence of cationic (cetyltrimethylammonium bromide) and non-ionogenic surfactants. The resulting NP solutions (5 – 6 nm, λ = 414 nm) were stable for several weeks. Photochemical reduction produced NP by mere illumination of a micellar solution with sunlight in the presence of atmospheric oxygen and dodecyl hepta(ethylene glycol) ether that acted as the micelle formation agent and the stabiliser. It was found that under the action of atmospheric oxygen, dodecyl ether of

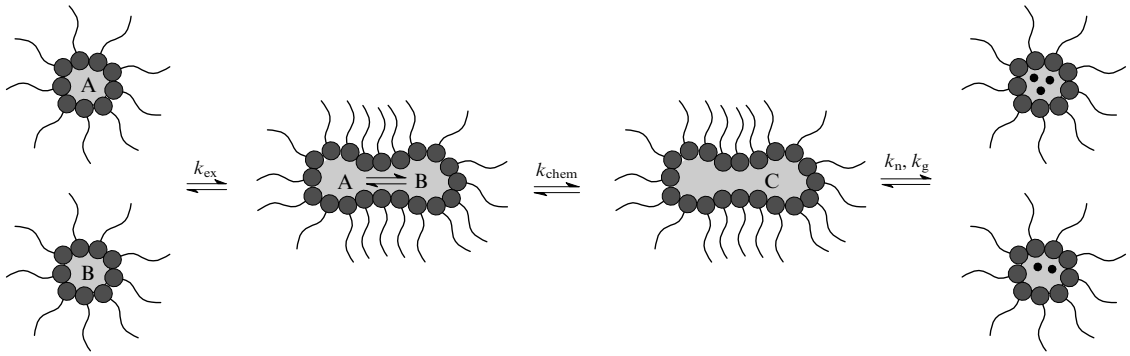
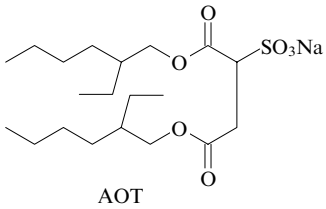


Figure 2. Mechanism of NP formation in inverse microemulsions.

hepta(ethylene glycol) produced a hydroperoxide that reduced Ag^+ ions.

Ternary systems hydrocarbon – water – AOT [AOT is sodium bis(2-ethylhexyl)sulfosuccinate] allow one to widely vary the water core diameter in a 'nanoreactor' by changing the molar ratio H_2O : AOT (AOT micelles can solubilise up to 60 water molecules per AOT molecule in a hydrocarbon medium). These systems proved to be extremely simple and suitable for the synthesis of silver NP with different diameters.



AOT

For $W_0 \leqslant 6$, all water in a micelle is involved in hydration of polar groups of surfactants and cannot be frozen; for $W_0 \geqslant 15$, the radius of a micelle water core is directly proportional to the water content in it ($r_w = 1.5\,W_0$).[76] The detailed description of properties of surfactants capable of inverse micelle formation can be found in a review.[77] Systematic studies [78, 79] of the NP formation in ternary systems hydrocarbon – water – AOT employed silver bis(2-ethylhexyl)sulfosuccinate as both the silver source and a co-surfactant.

Due to the diphilic nature of AOT (like of any other surfactant), NP stabilised by it are soluble in either polar or non-polar solvent depending on the method of synthesis. This is also true for the majority of so far known syntheses of nanosilver. At the same time, one often faces a problem of synthesising nanoparticles that would simultaneously satisfy certain requirements to their diameter, morphology and size and polarity distributions, because it appears that the synthesis of, *e.g.*, hydrophobic structures with the target morphological and size parameters requires the use of methods that utilise polar media and *vice versa*. This is why considerable attention was also paid to the development of methods of polarity reversal and the subsequent phase transfer of NP.[80–86] A simple and effective synthesis of silver NP with diphilic properties was proposed.[87] The synthesis was carried out in aqueous AOT solutions with different concentrations. The prepared hydrophilic NP could easily be extracted by cyclohexane in the presence of small amounts of phosphoric acid. After the solvent evaporation, silver NP were stable in the dry state and could equally easily be redispersed in either water or organic solvents.

The structure of NP in polar and non-polar media was studied [87] by the Fourier-transform IR spectroscopy (FTIRS). It was shown that the structure changes upon extraction. The role of phosphoric acid was not conclusively established; however, on the whole, the results correlated with the data of other studies.[88, 89] It was assumed that in the stabilising layer the polar groups of AOT molecules form a common system of hydrogen bonds with an H_3PO_4 molecule (or its anion). In an organic medium, the polar groups are oriented towards the nanoparticle surface, whereas in water, they are directed to the solvent. Thus, due to the described restructuring of the stabilising layer, the formed silver NP are of dual nature and can exhibit diphilic properties.

Mechanisms of silver NP growth in the inverse micelles formed by a non-ionogenic surfactant, namely, Triton X-100 [4-$Bu^tCH_2CMe_2C_6H_4O(CH_2CH_2O)_nH$, $n = 9-10$] were studied.[90] Nanoparticles were synthesised from different precursors {$AgNO_3$, Ag_2SO_4, $AgClO_4$, $[Ag(en)]^+$, $[Ag(CN)_2]^-$, $[Ag(NH_3)_2]^+$, $[Ag(edta)]^{3-}$, Ag_2O, AgBr, AgCl, AgOOCH} under the action of UV radiation. The mechanism and the kinetics of silver ion reduction were studied. It was found that the mechanism of NP growth was autocatalytic and substantially depended on the precursor type, particularly, on the nature of a constituent anion or a ligand. Thus the UV-radiation-induced reduction of micellar solutions proceeded by different routes for the first-group ($AgNO_3$, Ag_2SO_4, $AgClO_4$, AgCl, $Na[Ag(CN)_2]$) and second-group ($[Ag(NH_3)_2]^+$, Ag_2O, AgBr, AgOOCH) compounds. It is known that nanoparticles of noble metals (particularly, silver) exhibit extremely high photoactivity and are severely polarisable in UV light. As a result, the metal aggregates built of fine clusters acquire a positive charge, which leads to their instability and destruction to smaller constituents.[91] For first-type compounds, free Ag^+ ions were present in solution in a considerable concentration; this is why in the initial step, a large number of fine clusters were formed to quickly coagulate into coarser agglomerates ($\lambda = 480$ nm) (Fig. 3 *a*; steps *1* and *2*). Nuclei smaller that the critical size were thermodynamically unstable and dissolved, which favoured the growth of coarser particles (see Fig. 3 *a*, step *3*). In turn, the larger aggregates were unstable for photochemical reasons and disintegrated under UV radiation (see Fig. 3 *a*, step *4*). Thus, the formation of silver NP may be considered as a quasi-equilibrium process that includes parallel stages of growth and fragmentation to ultimately afford thermodynamically stable particles with a narrow size distribution. For second-type compounds, the bulk concentration of Ag^+ was small. In the initial step, only a few very fine clusters ($\lambda = 390$ nm) were formed (Fig. 3 *b*; steps *1*, *2*), hence, during the irradiation, slow processes of

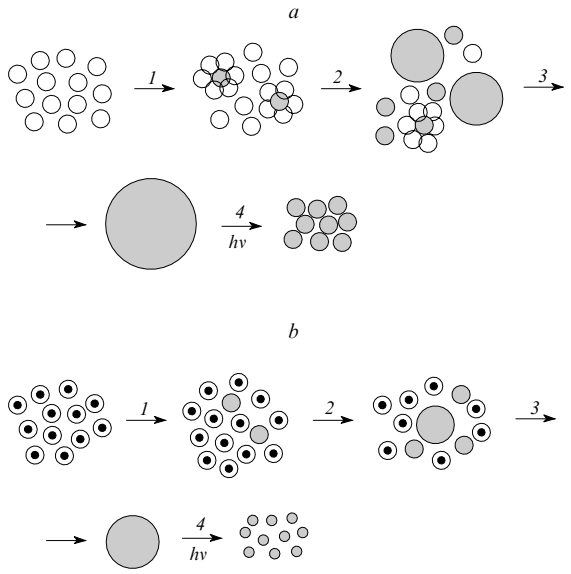


Figure 3. Different mechanisms of silver NP growth in inverse micelles and fragmentation under the action of UV radiation (see text).[90]
White circles (with and without a dot) are fine primary silver particles, grey circles are coarser NP.

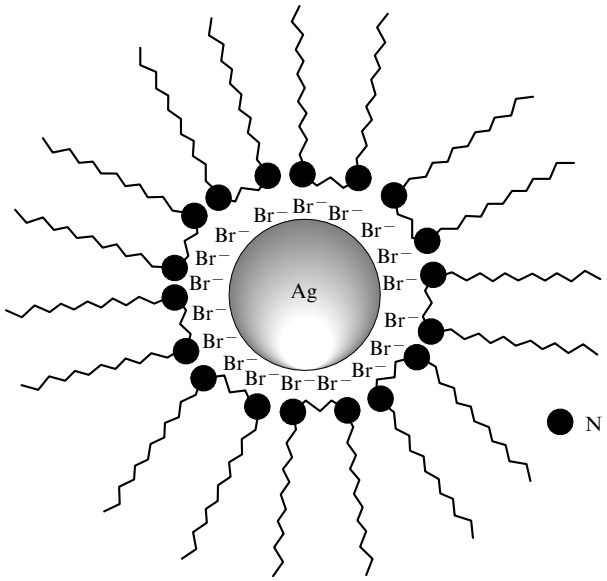


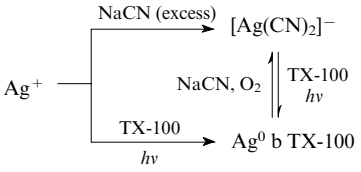
Figure 4. Illustration of a silver NP stabilised by a dimeric surfactant.[92]

aggregation of fine particles and fragmentation of coarser particles occurred, which also led to the thermodynamically equilibrium state. It should be noted that the second process afforded finer silver NP.

The reversible growth and dissolution of NP was simulated [90] in a sodium cyanide-containing system, where the silver NP formation was followed by their dissolution according to the equation

$$4\,Ag^0 + 8\,NaCN + O_2 + 2\,H_2O \longrightarrow 4\,Na[Ag(CN)_2] + 4\,NaOH.$$

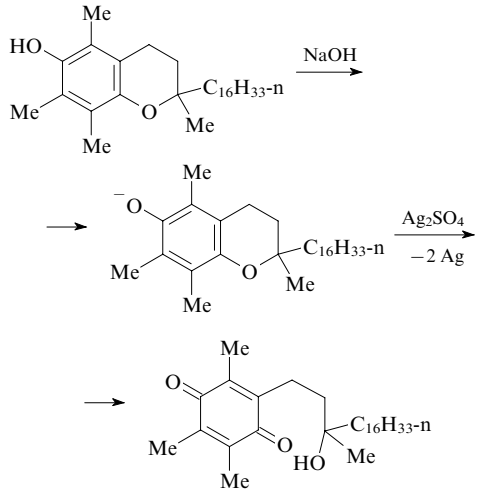
The choice of optimum reactant concentrations allowed a quasi-equilibrium state to be established, where the formation of NP with a narrow size distribution occured.



Recently, a dimeric surfactant, 2-hydroxy-1,3-bis(octadecyldimethylammonio)propane dibromide, was used in the synthesis of silver NP in inverse micelles.[92] The merits of dimeric surfactants include a low critical micelle concentration, their pronounced biological activity and enhanced solubilising capacity.[93] Effective stabilisation with dimeric surfactants made it possible to synthesise particles with a sufficiently narrow size distribution (7.1 ± 0.9 nm), which remained stable for many months (Fig. 4).

Advances in biotechnological methods of synthesis of natural surfactants [94] opened up the possibility of their use in environmentally clean syntheses of silver NP. Thus the properties of rhamnolipid, a natural surfactant, and its use in the synthesis of silver NP (2–8 nm) in inverse micelles were described.[95,96] Rhamnolipid may simultaneously act as an effective stabiliser of NP.

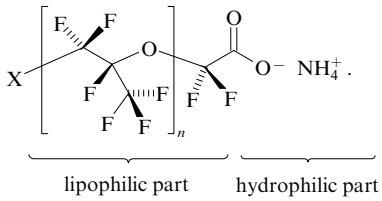
Synthesis of silver NP by the reduction of silver in Langmuir monolayers deserves mention,[97,98] where attention should be drawn to a method that employs the Langmuir monolayer (π = 20 mN m^{-1}, where π is the two-dimensional pressure) formed by α-tocopherol (vitamin E) molecules and a spread over the surface of aqueous solution of Ag_2SO_4 (Ref. 99). Tocopherol simultaneously served as the reducing agent and the stabiliser.



Ordered α-tocopherol molecules played the role of cluster nucleation sites and prevented their aggregation. Thus, the particle growth was localised and the growth of each individual particle was limited. The use of a minimum amount of reactants allowed the final product containing no impurities to be obtained.

As was noted above, a non-polar dispersion medium plays an important role in the formation of NP in micelles, affecting the kinetics of intermicellar exchange due to the different intensity of interaction of hydrocarbon 'tails' of surfactants with solvent molecules.[100–102] Hence, it appears tempting to control the properties of a dispersion medium in order to synthesise NP with target parameters. It is known that many characteristics of supercritical fluids and compressed gases,

such as density, diffusivity, dissolving capacity, compressibility, dielectric permittivity, *etc.* may be controlled by varying the temperature and the pressure. In turn, these properties can affect the extent of intermicellar exchange and the kinetics of NP growth. This is why supercritical fluids are utilised as the dispersion medium in micelle syntheses. For the first time, this method was used in the synthesis of aluminium hydroxide particles in supercritical propane.[103] Cason *et al.*[104,105] pioneered the synthesis of nanosilver (2–4 nm) in AOT inverse micelles in supercritical propane. The mechanism of NP formation and growth in supercritical fluids does not differ fundamentally from the mechanism of this process in liquid hydrocarbons under ordinary conditions. To compare the sizes of obtained silver NP, the latter were synthesised [104] in AOT inverse micelles with isooctane, cyclohexane and supercritical propane used as the dispersion media (temperature, reactant concentrations and W_0 were the same in all experiments, $P_{\text{cyclohexane}} = P_{\text{isooctane}} = 1$ atm, $P_{\text{propane}} = 200$ atm). It was found that in supercritical propane the formation of NP was completed in 20 min, whereas in cyclohexane and isooctane this took 50–60 min. This points to the higher intermicellar exchange rate in the first case to afford particles with the smallest diameter. Most of studies on the synthesis of nanosilver were accomplished in microemulsions in supercritical CO_2, because pure liquefied hydrocarbons are more expensive and dangerous in handling. A substantial drawback of liquefied carbon dioxide is its extremely low dissolving power with respect to the majority of surfactants including AOT and the instability of microemulsions based on it. This obstacle was overcome with the appearance [106–109] of perfluoropolyethercarboxylates with the general formula



Despite the inability of such polyethers themselves to form microemulsions with high W_0, the use of AOT as a cosurfactant allows overcoming this difficulty. The synthesis of silver NP (5–15 nm) carried out in a system containing AOT, perfluoropolyethercarboxylate, water and supercritical CO_2 was first described in 1999.[110] Later, the method was elaborated further.[111–115] SPR spectra of microemulsions recorded *in situ* [115] revealed peaks at $\lambda = 275$, 350, 380, 420, 470 and 530 nm, which corresponded to stabilised charged and neutral oligomeric silver clusters (Ag_4^{2+}, Ag_x^0, Ag_9^+, Ag_8^{2+}, *etc.*) and were retained for many hours. Such particles and their optical properties were described earlier.[116–118] The simultaneous involvement of water and perfluorinated polyether in stabilisation of silver clusters was inferred because no characteristic peaks were observed at $W_0 = 0$.

III. Unconventional syntheses of silver nanoparticles

The most often used chemical syntheses of silver NP in solutions have an essential flaw, namely, the necessity of using surfactants and stabilisers in the course of synthesis and impossibility of complete cleaning of the NP surface from these chemicals. This also concerns their contamination with boron, nitrogen and carbon compounds, associated with the use of reducing agents. At the same time, in the majority of applications of silver NP such as microelectronics, medicine, spectroscopy and catalysis, the presence of even trace amounts of impurities is harmful. Hence, the synthesis of chemically pure NP of noble metals is a challenge for scientists, and versatile and highly effective methods for cleaning nanomaterials must be developed in the immediate future.

1. Laser ablation method

Syntheses of silver NP that employ a minimum number of reagents, sometimes, only pure solvent, can be carried out by laser ablation of either bulk metal silver samples in liquid media [119–125] or microparticles in aerosols.[126–128] Figure 5 illustrates a unit for laser ablation.

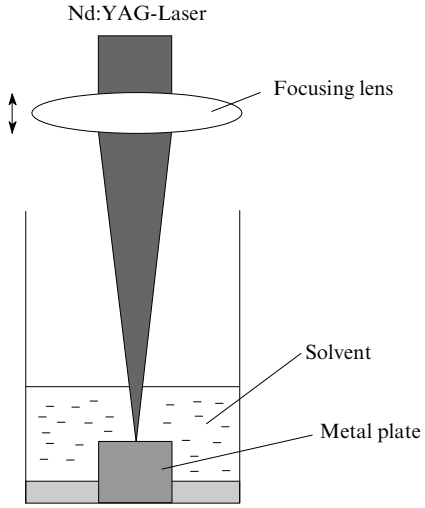


Figure 5. Scheme of a unit for laser ablation in liquid media.[129]

Laser ablation of a silver plate made it possible to synthesise [125] non-modified spherical silver NP with a logarithmically normal size distribution (Nd:YAG-laser, $\lambda = 1064$ nm, $t_{\text{pulse}} = 9$ ns, $I = 10$ J cm^{-2}, $\nu = 10$ Hz, where t_{pulse} is the pulse time, I is the radiation power, ν is the frequency) in acetonitrile (the average diameter of particles $d_{\text{av}} = 1.9$ nm), DMF ($d_{\text{av}} = 2.2$ nm), THF ($d_{\text{av}} = 2.4$ nm), DMSO ($d_{\text{av}} = 3.9$ nm).

According to absorption spectra of samples (Fig. 6) and their micrographs taken by high-resolution transmission electron spectroscopy, the particles prepared in THF and DMSO were covered with a nanometre shell of amorphous carbon, which was the thickest for DMSO. Particles with 'bare' surfaces were shown to exhibit sufficient aggregative stability due to their stabilisation by solvent molecules and easily underwent functionalisation with n-dodecane thiol and thioctic (α-lipoic) acid. Much earlier, silver NP were synthesised [129] by laser ablation in an aqueous sodium dodecyl sulfate solution. The number of NP formed was proportional to the radiation power and their average size increased with both an increase in the laser power and a decrease in the surfactant concentration. These trends were explained in terms of a model of fast formation of fine silver clusters and their subsequent growth competitive with the surface blockage by sodium dodecyl sulfate. This allowed an equation to be derived that

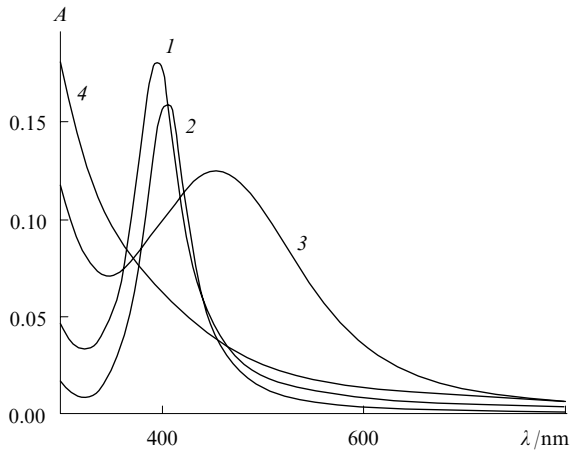


Figure 6. Absorption spectra of silver NP synthesised by laser ablation in acetonitrile (*1*), DMF (*2*), THF (*3*), DMSO (*4*).[125]

linked the average particle size with the experimental parameters.

Another approach to the synthesis of silver NP [126] included laser irradiation of an aerosol formed by silver microparticles (1.5 ± 0.2 μm) in nitrogen. In the laser ablation of microparticles, the nanoparticles were formed by a different mechanism (as compared with ablation of bulk samples). In the majority of processes that included steps of NP nucleation, aggregation and subsequent growth, the NP size distribution usually obeyed the logarithmically normal law. The considered method included fast laser-induced heating of microparticles, accompanied by the metal evaporation from the particle surface. As the atoms continue to be evaporated and then ionised, the microparticle disintegration starts, generating a shock wave opposed to the laser beam. This shock wave collides with a shock wave generated by the laser beam inside a particle and directed towards its centre. The collision heats the material to the critical temperature and initiates the so-called catastrophic condensation of atomic vapour, which leads to the local formation of NP in the low-pressure region in the vicinity of the shock wave route. As a result, a nanomaterial with a bimodal size distribution of particles was formed. The first (finer) fraction corresponds to NP formed as a result of shock wave-initiated catastrophic condensation, the second fraction contained particles formed in the vapour condensation as a result of initial heating of microparticles before the destruction step.

2. Radiolytic methods

Radiolytic methods based on the impact of electrons or high-energy γ-radiation on samples were used in the synthesis of silver clusters and the investigation of their properties and mechanisms of formation for quite a long time.[18, 117, 130–133] Above, the fundamental experiments by Henglein and Ershov were discussed that included the use of the pulse or γ-radiolyses in studying the mechanisms of growth and stabilisation of silver NP. The advances of recent years have shown that radiolytic methods represent a very promising way of preparative synthesis of silver NP.[134] This is explained by the possibility of smooth regulation of the radiation intensity, its rate and the exposure time thus exerting effective control over the reduction processes in the reaction system. Moreover, this eliminates the use of conventional reducing agents and, in certain cases, stabilisers, the excessive presence of which contaminates the final product. This approach may be exemplified by a study [135] in which metal clusters were formed in the presence of only a precursor and a solvent. The reduction of $AgClO_4$ in the water–ethylene glycol system involved the use of pulse radyolysis with 7 MeV electrons. An increase in the ethylene glycol content substantially increased the silver NP yield and their average diameter, namely, d_{av} was 70 nm in 1% ethylene glycol solution in water and 17 nm in 1% water solution in ethylene glycol. This was associated with widely different work functions of solvated electrons in pure water (2.9×10^{-7} mol J^{-1}) and ethylene glycol (1.7×10^{-7} mol J^{-1}) [136] and with the increase in the solution viscosity. The latter confirms that the reaction of solvated electrons with silver ions in pure water and ethylene glycol is diffusion-controlled.[130] A peak observed at 390 nm was assigned to the Ag_2^+ cluster with adsorbed ethylene glycol molecules, which confirmed the stabilisation of metal clusters by ethylene glycol molecules.

The possibility of using of amorphous silica particles as the stabiliser of silver NP formed in radiolysis was studied. [137–140] In one of these studies,[140] 1% aqueous Aerosil suspension (S_{sp} = 337 m^2 g^{-1}) with the primary particle size of 7 nm was used. According to the microscopic and X-ray diffraction studies, the product represented silver NP with the diameter of 10–20 nm adsorbed on the surface of Aerosil aggregates. An interesting method of controlling the particle size was proposed.[141] Aminopolysaccharide chitosan (0.02% solution in 1% acetic acid) employed as a stabiliser decomposed under the action of γ-radiation, where the degree of decomposition depended on the radiation dose. For the absorbed dose of 30 kGy, NP with the average diameter of 4–5 nm were obtained, because under these conditions, the chitosan chains were virtually unaffected by the destruction and could effectively stabilise the formed clusters. For larger doses (100 kGy and higher), low-molecular fragments of disrupted chitosan macromolecules were formed; under these conditions, coarse NP with a wide size distribution were formed.

3. Vacuum evaporation of metal and the Svedberg method of electrocondensation

Nanoparticles can be synthesised directly from silver atoms formed in the metal evaporation. Metal vapour was obtained by vacuum evaporation [142–146] or by passing a high-frequency (800–900 kHz) discharge through a layer of an organic solvent containing metal powder.[147] The latter method is known as the Svedberg electrocondensation.[148, 149] Both methods generate extremely reactive metal atoms that tend to pass into a more stable state.

Evaporation in high vacuum produces a gas that consists of metal atoms, which are later condensed with an excess of an inert gas on a cold (4–77 K) substrate. Even at such low temperatures, fine metal clusters (dimers, trimers) with characteristic absorption bands in the UV, visible and IR spectral ranges were formed. Subsequent heating of this system above the inert gas boiling point resulted in the irreversible growth of clusters to afford submicron particles; hence, this method is of no practical importance. Preparative amounts of metal NP can be obtained in the vacuum evaporation of a metal followed by low-temperature (77 K) co-condensation with excess vapour of an organic solvent. This method of NP synthesis is called the solvated metal atom dispersions (SMAD); its rapid development was observed in the late 1970s–early 1990s.[150–154] At present, a substantially smaller number of publications are devoted to this issue. This is associated, first, with reaching a

limit in the development of basics of this method that corresponds to the modern level of experimental instrumentation and, second, with the complexity of equipment and the highly expensive synthesis, which hinders its extensive use in practice.

In the 1960s, a synthesis of highly dispersed metals in polar and non-polar organic solvents was developed,[155, 156] based on the Svedberg method, namely, the use of pulsed high-frequency spark discharge induced between metal particles in an organic medium. Under these conditions, dispersion of a metal represents a condensation process, namely, under the action of a discharge, the metal is evaporated, which is followed by condensation of vapour in the solvent bulk. The NP size is stabilised as a result of interaction of surface metal atoms with the organic phase components. Substantial reduction in the average size and enhancement of the stability of dispersions may be achieved by adding surfactants to the system. This method makes it possible to prepare stable (for more than 6 months) NP sols in oxygen-containing solvents such as acetone or ethyl acetate.[155] The average particle size in the silver–acetone system was 1.5 nm. In non-polar media (heptane, octane, benzene, toluene), a stabiliser, particularly, caoutchouc or aluminium salts of organic acids, were introduced into the system. This method is substantially simpler than the vacuum evaporation of metals as regards both the equipment and the experimental procedure. Its disadvantage concerns the decomposition of the organic solvent during the discharge.

4. Biosynthesis of silver nanoparticles

The existence of microorganisms capable of biomineralisation, *i.e.*, production of inorganic materials,[157–160] and biodegradation of heavy metal salts [161] was known for quite a long time. The development of experimental methods of NP production and the extension of NP application fields (especially in medicine) necessitated the elaboration of environmentally clean syntheses of these particles based on the biotechnology achievements that rule out the use of toxic reagents. In 1999, the information on the intracellular biosynthesis of nanosized silver objects, which was performed using a bacterial strain *Pseudomonas stutzeri* AG259, was published.[162] The cell growth in the presence of Ag^+ was found [162, 163] to be accompanied by the formation of polyhedral silver crystals with the average diameter of 100–200 nm in the periplasmic space of cells. The mechanism of NP formation is still unclear; however, proteins with affinity for silver and containing fragments capable of acting as the nucleation sites were assumed to play a certain role. The intracellular synthesis of silver NP with the average diameter of 25 ± 12 nm was carried out in the growth of the strain of the AAT-TS-4 fungus *Verticillium*.[164] This process afforded metallic silver rather than its sulfide, which makes improbable the involvement of glutathione and other sulfur-containing peptides in this process in contrast to the biosynthesis of CdS (Ref. 165) and Ag_2S (Ref. 166). Despite the fact that most NP in the final product turned out to be immobilised on the cell walls, the reduction was assumed to proceed by an extracellular mechanism. Probably, Ag^+ ions were initially adsorbed on the mycelium film of a fungus cell due to electrostatic interactions and then underwent enzymatic reduction, which involved proteins from the cell wall structure. The further growth of a formed cluster proceeds through the reduction of Ag^+ ions on its surface.

It was shown recently [167] that *Fusarium oxysporum* fungus species are capable of extracellular reduction of aqueous silver nitrate solutions to afford metal NP with the diameter of 20–50 nm. The mechanisms of silver ion reduction by different strains of *Fusarium oxysporum* were studied.[168] Nanoparticles (20–50 nm) prepared in the extracellular synthesis employing the *Fusarium oxysporum* strain 07SD demonstrated intense absorption at 415–420 nm; their aqueous dispersions exhibited very high stability for several weeks. According to scanning electron microscopy data, silver particles were not in direct contact with one another even in aggregates, which pointed to their stabilisation by high-molecular species. Fluorescence ($\lambda_{max} = 340$ nm) and visible absorption ($\lambda_{max,1} = 265$ nm, $\lambda_{max,2} = 415$ nm) spectra of NP solutions have shown that stabilising proteins contained tryptophan and tyrosine and were in their native form.

Similar results were obtained in the reduction of silver nitrate solutions in aqueous phase filtrates containing *Fusarium oxysporum* 07SD, which pointed to the extracellular mechanism of reduction. The results of thin-layer chromatographic and fluorescence spectroscopic studies of these solutions revealed the presence of 2-acetyl-3,8-dihydroxy-6-methoxyanthraquinone or its isomer, 3-acetyl-2,8-dihydroxy-6-methoxyanthraquinone, *i.e.*, the well known extracellular electron carriers,[169] and the presence of NADP-dependent nitrate reductase. The latter was contained in all studied *Fusarium oxysporum* strains. It was shown that *Fusarium moniliforme* failed to reduce Ag^+ ions although evolved nitrate reductase into the medium; however, *Fusarium moniliforme* did not evolve anthraquinones but formed only naphthoquinones that act as extracellular electron carriers. Thus, the probable mechanism of silver reduction includes the conjugated oxidation–reduction reactions of electron carriers in which NADP-dependent nitrate reductase takes part (Fig. 7).

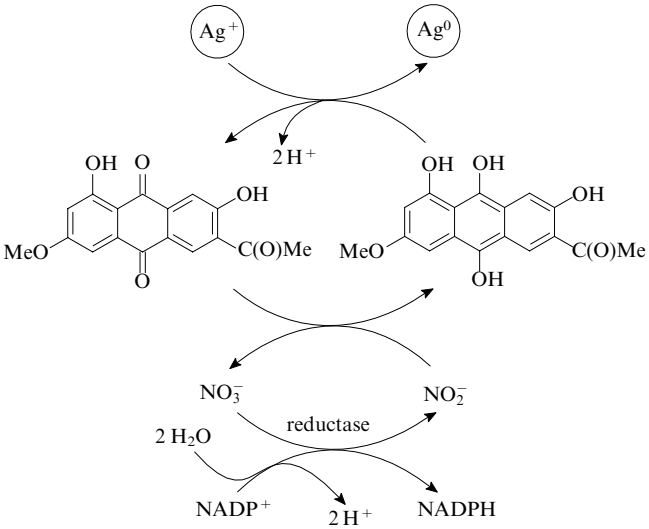


Figure 7. A probable mechanism of extracellular reduction of silver ions by a strain of fungus *Fusarium oxysporum*.[168]

An *in vitro* biosynthesis of silver NP, which involved α-NADP-dependent nitrate reductase, was modelled.[170] The reduction was conducted under anaerobic conditions in the presence of α-NADPH has a cofactor, a protein phytochelatin (NP stabiliser), 4-hydroxyquinoline (electron carrier) and nitrate reductase (with the molecular mass of 44 kDa) from *Fusarium oxysporum*. This afforded a dispersion of silver NP measuring 10–25 nm and stabilised by phytochelatin (absorption maximum at 415 nm), which was stable for several months. Figure 8 shows the absorption spectra of solutions

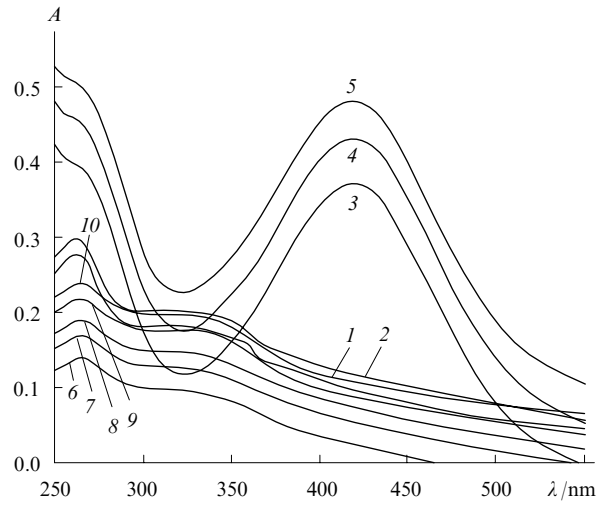


Figure 8. Absorption spectra of solutions after *in vitro* biosynthesis of silver NP (*1–5*) in the presence of all components and in the absence of (*6*) nitrate reductase, (*7*) α-NADPH, (*8*) phytochelatine, (*9*) 4-hydroxyquinoline, (*10*) with denaturated nitrate reductase.[170]
Reaction time /h: 1 (*1*), 2 (*2*), 3 (*3*), 4 (*4*) and 5 (*5*).

recorded after the synthesis carried out in the presence of all components and in the absence of at least one component. Apparently, the bioreduction of silver nitrate failed to proceed in the absence of even one component of the system. Thus, the presented data confirm the proposed [168] mechanism of silver NP biosynthesis. In should be noted that the extracellular synthesis has considerable advantages over the intracellular process, because in the latter case, NP must be separated from the biomass for their further use.

An Ag^+-resistant yeast strain MKY3 in the logarithmic growth phase was proposed [171] for the extracellular biosynthesis of silver NP with diameters of 2–5 nm. It should be noted that yeast grown in the absence of silver ions was incapable of the reduction. Apparently, the secretion of biochemical reducing agents by yeasts in their growth phase was associated with a sort of 'stress' towards introduced silver ions.[172] For preparative extraction of this material from large volumes, an original procedure of fractional melting was proposed, which is based on the trend of silver NP to be collected on the bottom of a vessel at -20 °C. At careful defrosting, the NP-containing layer melted at -8 °C and the rest of the medium melted at 1 °C, which forms the basis for their separation. The procedure was repeated several times in order to achieve the necessary degree of purity.

Biosynthesis of spherical, triangular and hexagonal silver nanostructures (60–150 nm) by the reduction of Ag^+ ions with oligopeptides selected by screening of their capability for selective binding to the surface of silver NP is documented.[173] A combinatorial approach based on selective recognition of inorganic substrates by peptide molecules that could later serve as the templates in the growth of these materials was described.[174–176] The directed growth of crystals of one or another form was governed by the selective interaction of peptides with individual facets. For example, a decrease in the surface energy of {111} facet as a result of its selective binding to a peptide made possible the growth of other crystal facets with lower initial energies. Thus, the surface interaction of a cluster nucleus with peptides determines the further selective growth of its individual facets.

Fundamental studies [177–179] of the role and the behaviour of cell membranes of microorganisms in their interaction with metals in ionic and colloid states were carried out. The cell response to the mentioned impacts was studied, including their effect on the physiological activity of intact cells. It was found that the interaction of these cells with metal NP exhibits pronounced selectivity.

IV. Shape-controlled synthesis of silver nanoparticles

In the past five to seven years, a new direction emerged associated with the preparation of non-spherical nanoobjects both planar (triangles, penta- and hexagons, circular plates, *etc.*) and three-dimensional (tetrahedra, cubes, prisms, rods, wires, *etc.*). Spherical particles that have the minimum surface for a given volume are thermodynamically more stable. If the reduction of univalent silver ions proceeds under thermodynamic control, its main products are spheres. However, in the course of synthesis, it is often possible to realise conditions favourable for kinetically controlled transformations that lead to non-spherical NP. As a rule, the following approach was used: in the initial steps of synthesis, 'primary' particles (nuclei) were formed under thermodynamic control, which was followed by their slow transformation into the final product under kinetic control.

The factors responsible for the anisotropic growth can be divided into the following two groups: 3D-diffusional and sorption factors. In the first case, the region of particle growth is spatially limited by environment components; in the second, the growth is blocked in certain directions as a result of selective sorption of a stabiliser on certain crystallographic facets.

1. Synthesis in micellar and spatially limited media

In a system water–non-polar organic substance–surfactant, at certain component ratios, not only spherical direct and inverse micelles but also ordered structures of different geometry, *e.g.*, layered, can be formed. When a silver salt is reduced in such media, the diffusion limitations determine the anisotropic growth of particles. Silver plates were obtained in organised media.[180] Prior to the reduction of silver ions with hydrazine, a mixture of n-octylamine and pentylamine was added to the aqueous phase in a ratio of 25 : 1. According to X-ray diffraction data, n-octylamine and water formed a layered structure that contained a $\sim$2.7 nm-thick aqueous layer and a surfactant double layer $\sim$1 nm thick. During the reduction, silver ions and reductant molecules were localised entirely in the aqueous layer. With respect to univalent silver ions, hydrazine acts not only as a reductant, but also as a complexing agent. This favours a decrease in the surface energy of metal nuclei. Dependences of the final size of particles (10–80 nm) on the silver ion content and the water-to-surfactant concentration ratio were studied.[180]

Lyotropic liquid-crystaline media can serve as templates in the synthesis of anisotropic silver nanoparticles. Thus the synthesis of nanowires with a large aspect ratio was carried out [181] in hexagonal liquid-crystaline phases formed by cylindrical inverse micelles containing long water channels.

A somewhat different approach was implemented [182] in the synthesis of monodispersed cubic silver NP measuring 55 ± 5 nm. This involved the use of the silver mirror reaction (aqueous solution of ammoniacal silver bromide and glucose) at high temperatures in the presence of cetyltri-

methylammonium bromide. Presumably, cubic NP formed due to the trend of CTMA towards anisotropic adsorption on silver crystal facets. An increase in the molar ratio CTMA : silver increased the yield of cubic nanocrystals.

A method of controlled single-phase synthesis of nanospheres, nanorods and nanowires based on the reduction of silver ions with sodium borohydride in the presence of DNA was proposed.[183] With the increase in the DNA content and the reaction time, the fraction of anisotropic particles (nanorods and nanowires) increased.

In the synthesis of anisotropic particles, not only 'soft' but also 'rigid' matrices were used. Silver nanotubes and nanorods were synthesised in the electrolysis of aqueous solutions of silver salts in a porous alumina matrix.[184, 185]

2. Methods for synthesising non-spherical objects based on kinetically controlled transformations

a. Processes that occur in the formation of non-spherical particles

Seed particles can undergo further transformations under the kinetic control. The main processes are the crystallisation of initially amorphous particles and their subsequent layer growth. Strong reducing agents such as sodium borohydride are conventionally used only in the formation of seed particle. The further slow growth of non-spherical nanoobjects is as a rule conducted in a medium containing organic reducing agents with hydroxyl or aldehyde functions. One compound often serves as both the reducing agent and the reaction medium (solvent). The most frequently used compound is ethylene glycol; this is why, in the literature, this direction is referred to as the polyol synthesis of NP.

In contrast to the fast reduction of univalent silver compounds to afford spherical nuclei measuring up to 10 nm, the crystallisation and, particularly, the layer growth of NP, is a slow process that takes considerable time. Its acceleration often involves the use of elevated temperatures (100 – 200 °C), *i.e.*, the process is often carried out in a boiling organic solvent. The inner ordering and growth of NP resemble the ageing of deposits known in inorganic and colloid chemistry. Ageing is accompanied by the inner structuring and growth of coarse particles and the destruction and 'dissolution' of fine particles. For particles with the size above a certain value, the former process occurs; for smaller particles, the latter process takes place. This value is called the critical nucleus size. In the formation of silver NP, such processes are intensified at 85 °C. At the same time, the critical nucleus size was observed to increase with the increase in the temperature.[186]

As the crystal structure of silver NP is formed, the selective dissolution of Ag^+ ions from individual facets becomes possible. For this purpose, a substance is added to the system that can selectively adsorb on certain crystallographic facets thus preventing their growth. As a result, the anisotropic growth of particles is observed. PVP was used most often as such an additive. However, this effect was also observed for polyacrylic [187] and ascorbic [188] acids, sodium citrate [189] and some other reagents. In all the cases, there is a region of optimal reagent concentrations such that for too low concentrations, the sorption insignificantly affects the growth processes, whereas for too high concentrations where non-selective sorption prevails, the metal reduction is inhibited on all crystal facets.

The morphology and size of particles substantially depend on the experimental conditions (temperature, silver salt concentration, $PVP : Ag^+$ ratio). For temperatures below 120 or above 190 °C, irregular NP prevailed in the products. When the silver ion concentration became lower than 0.1 mol litre^{-1}, nanorods were the main reaction product. As the molar ratio $PVP : Ag^+$ increased from 1.5 to 3, the preferential growth of particles that represented agglomerates of several single crystals started. For a high (0.25 mol litre^{-1}) initial concentration of silver ions and the reaction time of 14 min, cubic nanoparticles measuring 95 ± 7 nm were formed. A slight increase in the reaction time (to 17 min) led to the formation of particles measuring 115 ± 9 nm. A decrease in the initial concentration of silver ions (to 0.125 mol litre^{-1}) favoured a decrease in the particle size. In this case, particles measuring 80 ± 7 nm were formed even after 30 min; moreover, somewhat finer particles (~ 50 nm) were formed in 25 min, albeit the latter were not totally (perfectly) cubic.[59]

b. Nanorods and nanowires

The growth of nanorods may proceed under kinetic control.[190] The process started with a decahedral nucleus formed by tetrahedral clusters that share facets. Insofar as the dihedral angle in a tetrahedron is $\sim 70.5°$, a decahedron (pentagonal pyramid) that consists of five tetrahedral fragments is one of the most thermodynamically stable forms of such multiply twinned particles (MTP) (Fig. 9 *a*). Structures with such geometry were discovered and described by Ino and Ogawa.[191, 192] It should be noted that the dihedral angle in a tetrahedron is slightly smaller than $2\pi/5$ (72°); hence, the tetrahedra cannot be ideally packed into a decahedron without gaps (structure defects). The information on the experimental studies of the structure of the finest particles including the synthetic conditions and the structure of multiply twinned particles can be found in a review.[193]

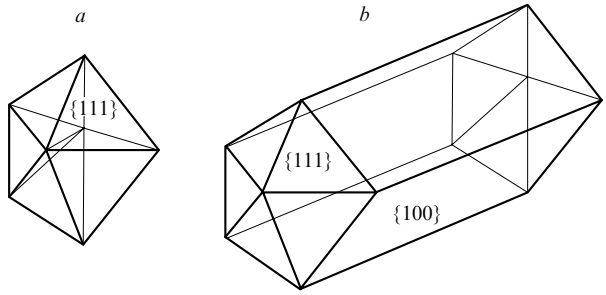


Figure 9. Scheme of growth of a silver nanorod. (*a*) decahedral nucleus; (*b*) nanorod.

The formation of nanorods and nanowires is the result of anisotropic growth of nuclei along a five-fold symmetry axis. In the decahedron growth, the formation of a next atomic layer on structure defects involves the formation of {100} facets. PVP molecules selectively adsorb on these facets blocking their growth.[189] As a result, the particle growth proceeds solely in the direction of crystallographic planes {111} to afford nanorods with pentagonal pyramids formed by {111} faces at their ends and PVP-blocked {100} faces at their side surfaces (Fig. 9 *b*). Based on the aspect ratio ($a = l/d$), all objects can be divided into the following four groups:[190] NP ($a \approx 1$), short nanorods ($a < 5$), long nanorods ($5 < a < 25$) and nanowires ($a > 25$). A tetrahedral silver particle is limited by the {111} planes that are apparently retained in a nucleus of decahedron. A decrease in the initial concentration of univalent silver ions favours the formation of particles with larger l/d ratios. For a larger ratio of PVP and Ag^+ concentrations ($\geqslant 18$), no nanorods were formed, whereas for low ratios ($\leqslant 1.5$), nanorods

were the main product. The addition of ascorbic acid to the original mixture favoured the formation of uniform (in size) nanorods and nanowires with the reproducible l/d ratios.[186]

Not only silver particles can serve as the seeds of nanorods and nanowires. A two-step synthesis of nanowires in which platinum NP were used as the growth sites of silver crystals was described.[194] In the first step, platinum(II) chloride was reduced in the ethylene glycol medium at 160 °C after which solutions of PVP and silver nitrate in ethylene glycol were introduced into the system without cooling.[194] A decrease in the concentration of primary platinum nuclei led to a decrease in the nanowire diameter.[186] According to data from electron microscopy, the growth of one-dimensional structures starts between the tenth and the twentieth minute, while the formation of particles with the l/d ratio >100 took no less than 60 min. Particles measuring <5 nm were formed on silver nuclei, whereas objects with the diameter of 20–30 nm were formed on platinum nuclei. The presence of PVP can have a pronounced effect on the geometry of coarse particles due to the selective adsorption on different facets of silver single crystals, which determines the shape anisotropy during the growth.[189] Whereas the formation of primary particles was sufficiently fast (about one or several minutes), the secondary growth took 20–60 min.

The slow dissolution of fine primary silver particles may also affect the formation of anisotropic particles. Platinum nuclei and PVP play the key role in the formation of nanowires. Electron diffraction on nanowires revealed the presence of a face-centred cubic structure with the cell parameter of 4.08 Å and the predominant content of {111} facets.[189] The relative content of nanowires strongly depended on the synthesis temperature. Thus, at temperatures below 100 °C, virtually no nanowires were formed.[194] The synthesis of silver nanorods by a two-step method that involves the use of platinum or silver nuclei was described.[186] Its scheme is similar to that of the nanowire synthesis with some deviations in the experimental conditions. In the first step, platinum and silver salts were reduced with ethylene glycol to form metal nuclei. Then, solutions of $AgNO_3$ and PVP were introduced. As a result, NP measuring 20–30 nm were formed. The nucleation on silver seeds led to the formation of NP with the diameter of 1–5 nm. No further growth occurred due to the presence of a sufficient amount of PVP in the reaction mixture.

The above methods of synthesis made it possible to develop the simple and reproducible procedures for the formation of nanowires with the target length.[195]

c. Nanocubes

The properties of compounds capable of selective adsorption on different crystallographic faces of silver single crystals are manifested most clearly in the synthesis of cubic particles. The slow growth of silver particles (single crystals) was studied [189] in the course of their polyol synthesis. A prerequisite for the synthesis of nanocubes is a relatively high (0.125–0.25 mol · litre^{-1}) initial concentration of silver ions, which provides the formation of single-crystal cuboctahedral nuclei. In the initial steps, cubic particles were formed as a result of preferential growth along crystallographic planes {111} of a cuboctahedron, which was explained by the selective adsorption of PVP molecules on {100} facets. After the formation of cubic metal particles was completed, their further growth was possible by the deposition of layers of metal atoms or small planar particles on the cube facets. The size of cubic NP could be varied in the range of 80–175 nm by varying the concentration of the starting silver compound.

d. Nanoprisms, nanoplates, nanobelts

Under certain conditions, the reduction of univalent silver compounds affords planar objects, namely, nanoprisms, nanoplates and nanobelts. The growth of nanoprisms and nanobelts starts with the formation of planar triangular nanoprisms. In essence, a triangular nanoprism represents a cross section of a cube cut in parallel to the {111} plane (Fig. 10). Triangular prisms can later transform into polyhedral plates either symmetrical (circular) or anisotropic (belts).

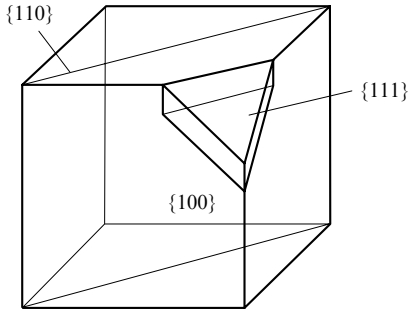


Figure 10. The main crystallographic planes in a cubic system crystal.

Nanoplates were preferentially formed when the silver crystal growth was preferentially blocked in the directions [111]. This was achieved by the addition of PVP and sodium citrate to the reaction mixture. Sodium citrate plays the key role in this system. In its presence, triangular prisms that form the basis of nanobelts and planar plates of different geometry (most often, circular) are formed. A synthesis of silver NP with controlled morphology was described.[196] For citrate concentrations above 0.1 mol · litre^{-1}, nanoprisms were the main reaction product. For lower concentrations, trigonal and hexagonal structures with a wide size distribution were formed. An increase in the longitudinal size of particles was usually accompanied by a slight increase in their thickness.[189] A series of samples of silver nanoplates with the thickness of $\sim$30 nm and the average diameter from 25 to 1000 nm were synthesised.[197] X-Ray diffraction studies revealed a single peak of the {111} plane. Silver nanodisks were synthesised in high yields by liquid-phase reactions.[198] Their two-step synthesis included the formation of triangular nanoplates (nanoprisms) and their ageing at 40 °C for 4 h.

As was mentioned above, polymers containing hydroxyl terminal groups can also serve as ideal reducing agents for the kinetically controlled growth of metal nanostructures, *e.g.*, commercial PVP terminating in the hydroxyl group due to the involvement of water or hydrogen peroxide in polymerisation.[199] Poly(vinyl pyrrolidone) was also added together with sodium citrate to the reaction mixture in the reduction of silver nitrate with sodium borohydride.[200] The reaction products represented particles of virtually perfect triangular or hexagonal forms. An increase in the nanoprism yield was achieved due to photo-induced reactions [12] carried out in the same way as the common reduction of silver nitrate with sodium borohydride in the presence of a stabiliser [sodium citrate, dipotassium bis(*p*-sulfonatophenyl)phenylphosphine dihydrate]. The reaction was initiated by visible light quanta with the wavelength of 350–700 nm. In 70 h, the system changed its colour from yellow (typical of spherical particles) to green and, finally, to blue. Transmission electron microscopic studies have shown that the original spherical particles measuring 8.0 ± 1.7 nm

ultimately transformed into prismatic particles measuring 100 ± 15 nm. According to electron diffraction data, an individual prism represented a silver single crystal with the face-centred cubic lattice. Its upper and lower facets were formed by {111} planes.

Recently, a synthesis of nanobelts by the reduction of silver nitrate with ascorbic acid in the presence of sodium polyacrylate (Na-PAC) at 4 °C in an aqueous medium was described.[187] In some experiments, after the reactants have been mixed acetic acid was added. The reaction product represented nanobelts formed by layers of nanoplates with diameters from 60 to 100 nm and heights of 30–40 nm deposited on one another. X-Ray diffraction studies revealed the presence of silver single crystals with the face-centred cubic lattice. A region of Na-PAC concentrations optimum for the synthesis of nanoplates exists. For a concentration below 0.5 mg litre^{-1}, Na-PAC did not affect the structure. A concentration of 1.6 mg litre^{-1} favoured a substantial increase in the nanobelt yield. Its further increase to 160 mg litre^{-1} led to the formation of a submicron branched structure of NP with the thickness of 20–30 nm. This phenomenon was associated with the selective adsorption of Na-PAC on different crystallographic planes of metallic silver. In the range of intermediate concentrations, Na-PAC was strongly adsorbed on the crystallographic plane {111} and less strongly on the {211} plane. This increased the yield of [110]-oriented nanobelts.

V. Optical properties of silver nanoparticles

1. Interaction of light with silver nanoparticles

A characteristic feature of metal NP is their strong and specific interaction with electromagnetic radiation. Highly dispersed metal sols are as a rule intensely coloured; moreover, the sol colour depends on the particle size and differs in scattered and transmitted light. It is not by accident that the first practical application of NP dealt with the preparation of pigments for the production of stained glass and ceramics.

Optical properties of silver NP strongly depend on the characteristics of both individual particles (their size, shape and composition and the presence of adsorption layers and their structure)[130, 201] and their environment including the spatial ordering of particles.[130, 202]

A characteristic feature of absorption and scattering spectra of metal NP with sizes above 2 nm is the presence of an intense and broad band in the visible range (Fig. 11) or in the adjacent near-IR and -UV ranges.

This band is called the surface plasmon resonance (SPR) band or, more frequently, the Mie resonance (after Gustav Mie who made the most considerable contribution to the theoretical interpretation of this phenomenon). Of all metals, silver has the greatest SPR band intensity; for gold and copper, the intensity it much weaker. Silver exhibits the highest extinction ratio in the SPR band peak among not only metals, but also the other known materials that absorb in the same spectral range (*i.e.*, in this spectral range, silver NP transmit light to the lesser extent as compared with any other particles of the same size).

The appearance of an SPR band is the result of the interaction of light incident on the NP surface with the conduction electrons of the metal.[203–205] According to the electron gas theory, the inner-shell (core) electrons are localised at the atomic nucleus, while electrons of the outer valence shells are free to move within a metal particle and be the reason of, for instance, high metal conductivity. Under the effect of the alternating electric field of a light beam, mobile conduction

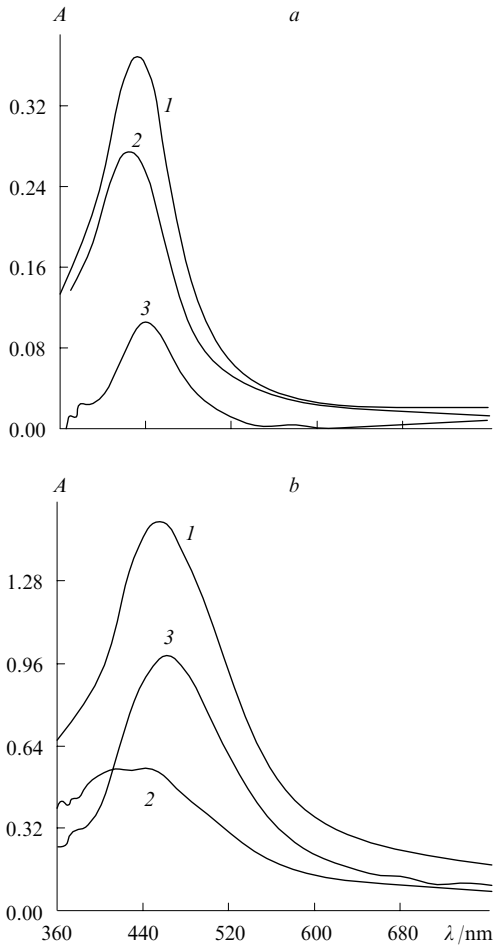


Figure 11. (*1*) Extinction, (*2*) absorption and (*3*) scattering spectra of silver NP with the average size of (*a*) 44 and (*b*) 76 nm.[23]

electrons are shifted. If the particle size is much smaller than the incident light wavelength, the electron motion leads to the appearance of a dipole (Fig. 12 *a*) that oscillates with the frequency of the exciting electric field.

If the frequency of incident light oscillations coincides with the intrinsic frequency of conduction electrons near the particle surface, then the resonance light absorption and scattering are observed, which is referred to as SPR. An oscillating dipole formed near the surface with a shift of conduction electrons is usually called a surface plasmon. For non-spherical particles or those located in a non-uniform environment, *e.g.*, fixed on a support,[206] the different orientations of particles with respect to the incident optical wave are non-equivalent. Thus for cylindrical particles, the surface plasmon resonance frequencies of dipole oscillations induced along and across the cylinder axis (Fig. 12 *b*) are different, which gives rise to two SPR bands in the spectrum.

The positive and negative charge regions formed near the NP surface as a result of a shift of conduction electrons result in polarisation of the environment in which the metal particle is located. Such polarisation reduces the amplitude and frequency of the induced dipole oscillations and, as a consequence, shifts the SPR band to longer wavelengths.[205, 207] These effects are the more pronounced for the stronger susceptibility of the medium to polarisation, *i.e.*, for the higher dielectric permittivity of the medium (ε_M).

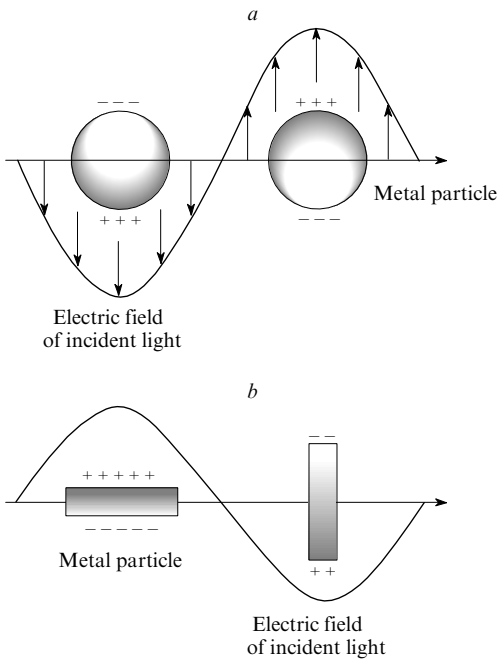


Figure 12. Interaction of electromagnetic radiation with metal particles (the particle size is much smaller than the incident radiation wavelength). (*a*) Spherical particle, (*b*) cylindrical particle.

To quantitatively calculate the peak position and the width of an SPR band, it is necessary to know the dielectric permittivity of silver (ε). In the general case, for an isotropic material, the parameter ε is a complex quantity and depends on the frequency of the variable electric field (ω)

$$\varepsilon(\omega) = \varepsilon_1(\omega) + i\varepsilon_2(\omega).$$

The non-zero imaginary part of ε is associated with the electric resistance of the medium and gives rise to a phase shift between the oscillations of the dipole and the electric field intensity. The function $\varepsilon(\omega)$ can be determined experimentally or calculated in terms of different models of the structure of the matter. Figure 13 shows the dependences of real and imaginary parts of the dielectric permittivity of silver on the wavelength of the incident radiation. As compared with other metals capable of exciting plasmon oscillations, silver has the lowest imaginary part of dielectric permittivity, which is responsible for the dissipation of the electric field energy. Hence, the efficiency of surface plasmon excitation in silver NP is the highest.

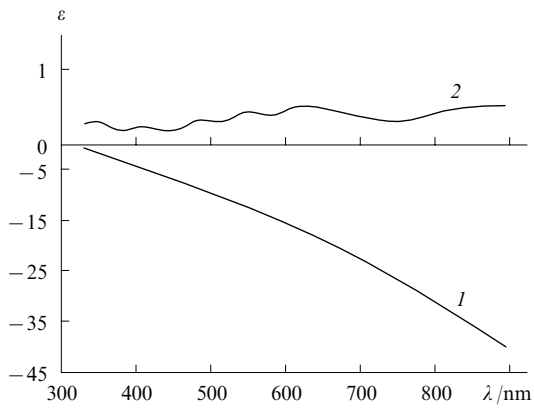


Figure 13. Dependences of the (*1*) real and (*2*) imaginary components of dielectric permittivity on the incident radiation wavelength.[23]

According to the Mie theory, the total cross-section of light absorption and scattering by a particle (C_{ext}) is

$$C_{ext} = \frac{24\pi^2 R\varepsilon_M^{3/2}}{\lambda} \frac{\varepsilon_2}{(\varepsilon_1 + 2\varepsilon_M)^2 + \varepsilon_2^2}, \quad (2)$$

where R is the particle radius, ε_M is dielectric permittivity of the medium (its real part; the imaginary part can be neglected in this derivation), λ is the incident light wavelength. Taking into account the fact that for silver, ε_2 depends weakly on the wavelength (see Fig. 13), then with the fulfilled condition $\varepsilon_1 = -2\varepsilon_M$, a resonance growth in the light absorption intensity is observed.

An essential advantage of the Mie theory is that the problem of calculating the absorption spectrum of a particle is divided into two independent parts, namely, the electrodynamic problem, which can be solved either exactly or (for particles of complex shapes) approximately, and a problem of finding the frequency dependence of permittivity.

According to formula (2), the dependence of a spectrum on the particle size shows up in the increase in SPR band intensity with the increase in the particle radius. Experimental data have shown that in addition to the increase in absorption, the growth of silver particles is accompanied by the SPR band broadening and the red shift of its maximum (Fig. 14).[23, 207, 208] At the same time, with an increase in the particle size, the SPR band of alkali metal NP shifts to shorter wavelengths. The effect of the particle size on the SPR band position and width was associated with the fact that dielectric permittivity of silver depends on the particle size.[130, 209] The particle size effect on the spectrum can be inversed due to the interaction of a silver particle with its environment, which includes the chemisorption on the particle surface.[210, 211]

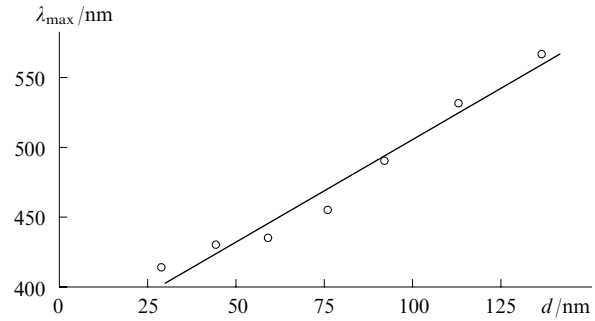


Figure 14. Position of an absorption band maximum as a function of the diameter of spherical silver particles.[23]

The Mie theory is consistent with experimental data for dilute silver sols and separate NP[212] where the interaction between dipoles belonging to different particles can be neglected. The major method used for the description of concentrated systems, namely, the effective medium theory, calculates the average dielectric permittivity of a medium that surrounds an individual particle by taking into account the spatial (3D) configuration of the particle. According to the Maxwell–Garnett model of effective medium, the dielectric permittivity of a medium with randomly distributed identical metal particles can be calculated based on the formula

$$\varepsilon_{\text{eff}} = \varepsilon_{\text{M}}\left(1 + \frac{3\phi\beta}{1-\phi\beta}\right), \text{ where } \beta = \frac{\varepsilon - \varepsilon_{\text{M}}}{\varepsilon + 2\varepsilon_{\text{M}}},$$

ε is the complex dielectric permittivity of a given metal and ϕ is the volume fraction of nanoparticles.

It should be mentioned that the above reasoning and calculations are suitable for the simplest case where an incident electromagnetic wave induces a dipole. The larger a particle, the higher the probability that systems with separated charges, namely, quadrupoles and other multipoles are formed. This is accompanied by the appearance of the corresponding additional SPR bands in the spectrum (Fig. 15). The contribution of quadrupoles into the overall light absorption becomes noticeable if the silver particle size exceeds 50 nm; for particles measuring 75 nm, the contributions of dipole and quadrupole resonances become equal.

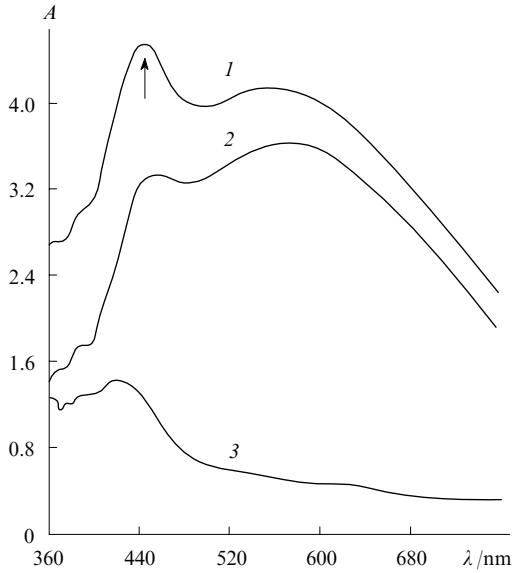


Figure 15. (*1*) Extinction, (*2*) scattering and (*3*) absorption spectra of silver NP with the diameter of 136 nm. The quadrupole SPR band is marked by an arrow.[23]

Gans applied the Mie theory to the calculations of a spectrum of cylindrical particles (nanorods) and arrived to the following expression for the overall cross-section of light scattering and absorption:

$$C_{\text{ext}} = \frac{2\pi V \varepsilon_{\text{M}}^{3/2}}{\lambda} \sum_j \frac{\varepsilon_2 / P_j^2}{\left[\varepsilon_1 + \varepsilon_{\text{M}}(1-P_j)/P_j\right]^2 + \varepsilon_2^2}, \qquad (3)$$

where V is the particle volume, P_j is the depolarisation factors for nanorod axes, j takes the values a, b and c, where a is the cylinder axis, b and c are the perpendicular diameters of the base ($a > b = c$). Depolarisation factors P_j are related to the particle size

$$P_a = \frac{1-r^2}{r^2}\left[\frac{1}{2r}\ln\left(\frac{1+r}{1-r}\right) - 1\right], P_b = P_c = \frac{1-P_a}{2},$$

where the supplementary parameter r is

$$r = \left[1 - \left(\frac{b}{a}\right)^2\right]^{1/2}.$$

As was mentioned above, in an absorption spectrum of cylindrical NP, two SPR bands are present that pertain to dipoles oscillating along and across the cylinder axis, *i.e.*, longitudinal and transverse plasmons, respectively. As follows from formula (3), with an increase in the cylinder length at a fixed diameter of its base, the absorption band of a longitudinal plasmon shifts to shorter wavelengths and its intensity decreases, whereas the SPR band of a transverse plasmon shifts to longer wavelengths and its intensity increases.

Certain peculiarities were observed upon the interaction of light with severely elongated metallic nanorods ($a \gg b$), *i.e.*, nanowires with the length comparable or exceeding the incident light wavelength. It this case, the intensity of the incident light-induced electric field substantially differs at the ends of a wire; thus, a dipole induced at one end polarises the adjacent nanowire areas and, in place of a spatially localised oscillating dipole, a travelling wave emerges on the metal surface and propagates from one nanowire end to the other.[213] A similar wave, which is usually called the surface plasmon polariton (SPP), was formed under the action of light on a chain of silver nanospheres in contact with one another. If light is directed to only one end of a nanowire (this is feasible for, *e.g.*, laser irradiation), then upon reaching the other end of nanowire, the travelling wave induces an oscillating dipole that emits light of the same wavelength as the incident light. Thus, silver nanowires and chains of nanospheres can serve as effective waveguides in optical nanodevices.[214, 215]

On going to particles with shapes more complex than spherical or cylindrical, the solution of the Maxwell equations becomes even more complicated; hence, the calculations of spectral characteristics require the use of different approximations and numerical methods.[216] The discrete dipole approximation (DDA) and the finite difference time domain method (FDTD) that allow one to calculate spectra of both individual silver NP (Fig. 16) and their ordered groups in different surroundings were applied most extensively.

The FDTD method is based on the substitution of finite differences for all derivatives involved in the Maxwell equation including the time derivatives. This allows one to substantially simplify the numerical calculation of the electric field intensity.

In the discrete-field approximation, a particle and its environment are split into unit cubic cells. For cells with sizes

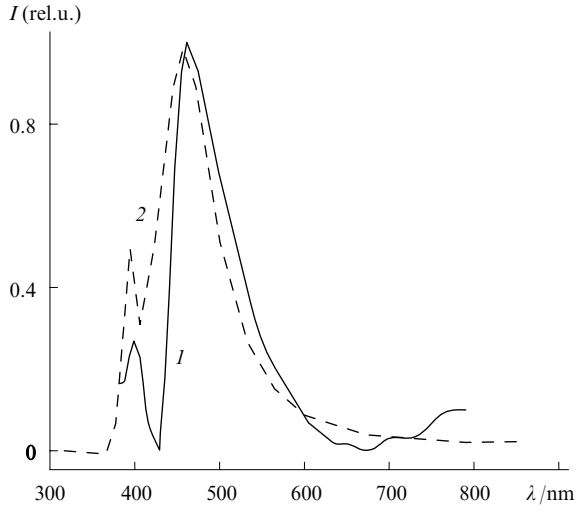


Figure 16. Absorption spectra of a glass-supported silver nanocube with 36 nm edges: (*1*) calculated by the FDTD method and (*2*) experimental.[206]

much smaller than the incident light wavelength, each cube can be considered as a dipole and the induced multifields are ignored. The intensity of an electric field that acts on a unit cube is calculated as a vector sum of intensities of a field generated by incident electromagnetic radiation and fields induced by the other cubes. Then, using different numerical methods, the electric field evolution in cells is calculated. The discrete dipole method allows exact calculation of local electric fields near a silver particle [217] and agrees well with experimental data.[218]

The absorption peak in the spectra of non-spherical silver NP is usually shifted to longer wavelengths; moreover, the wider the deviations in the particle shape from spherical the greater the absorption band shift (Fig. 17). Moreover, spectra of non-spherical particles show almost in all cases several SPR bands [219] caused by non-equivalent particle orientation with respect to the incident light wave.

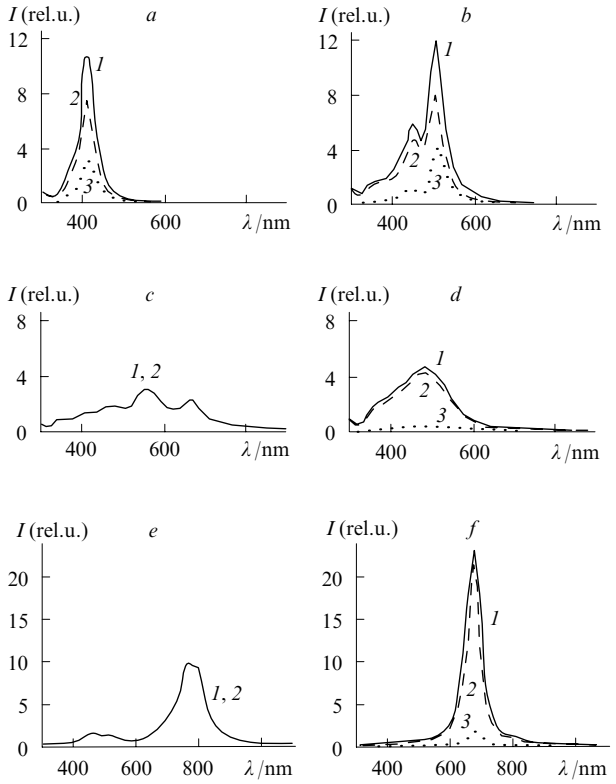


Figure 17. (*1*) Extinction, (*2*) absorption and (*3*) scattering spectra of silver NP with different geometry, calculated by the DDA method.[217] (*a*) Spheres with diameter of 40 nm; (*b*) cubes with edge length of 40 nm; (*c*) tetrahedra with edge length of 40 nm; (*d*) octahedra with edge length of 40 nm; (*e*) regular triangular prisms with base edge length of 40 nm and height of 5 nm; (*f*) disks with diameter of 40 nm and thickness of 5 nm. For (*c*) and (*e*), the scattering is virtually zero.

A change in the NP shape, particularly, the appearance of sharp corners leads to the greatest changes in the absorption spectra. Thus in the DDA-calculated [217] spectrum of silver nanospheres with diameters of 40 nm, the absorption band peak was at 420 nm. In the spectra of various silver polyhedra with edge length of 40 nm, the absorption maximum was in the vicinity of 500 nm for nanocubes and nanooctahedra and about 550 nm for nanotetrahedra. An even greater shift was observed for planar silver nanoobjects, namely, up to 700 nm for nanodisks (cylinders 40 nm in diameter and 5 nm in height)

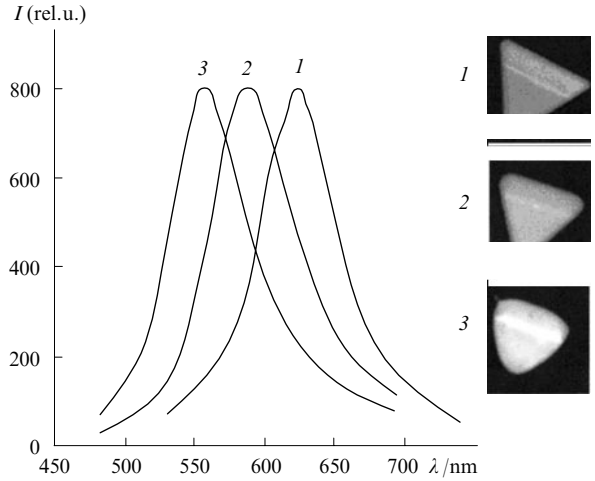


Figure 18. Scattering spectra of regular and rounded silver polyhedra.[218]

and 780 nm for nanotriangles (a triangular prism with 40 nm edges and 5 nm height). Such effects were also observed in spectra of silver nanorods and nanowires when their shape changed from circular to triangular.[220] Even a slight rounding of sharp corners, which left the overall shape of particles virtually unchanged, resulted in a blue shift of the SPR band to approach a spectrum of spherical particles. The theoretical calculations described above are well consistent with the scattering spectra recorded for regular and rounded silver nanotriangles (Fig. 18).[218]

2. The effect of surface plasmon resonance on optical characteristics of the near-surface layer

As was already mentioned in Section V.1, a shift of conduction electrons on illumination of a silver particle leads to the appearance of positively and negatively charged space regions. In the vicinity of these regions, the electric field intensity (E_{ind}) exceeds, by a large factor, that of the field (E) generated by a light wave incident on a particle

$$E_{ind} = \frac{\varepsilon - \varepsilon_M}{\varepsilon + 2\varepsilon_M} E ,$$

where ε and ε_M are the complex dielectric permittivities of silver and the medium in which the particle in located. The highest plasmon field intensity is reached when the exciting radiation frequency coincides with the SPR frequency (for $\varepsilon = -2\varepsilon_M$). Thus, in addition to the incident wave field, the molecules of a substance located on the particle surface experience a surface plasmon field that oscillates with the same frequency. As a result, the probability that light will interact with these molecules, *e.g.*, through photoluminescence, absorption or scattering, increases. The transition of molecules adsorbed on the particle surface into their excited state may selectively passivate and depassivate different areas on the silver particle surface.[221]

a. Surface-enhanced Raman scattering

Enhancement of Raman scattering near a metal surface was first observed in 1974 when studying the Raman spectra of pyridine adsorbed on a rough silver electrode.[222] The intensity of spectrum bands increased $10^5 - 10^6$-fold per molecule as compared with the Raman spectrum of pure pyridine.[219, 223]

Later, surface-enhanced Raman scattering (SERS) was observed for many molecules adsorbed on rough surfaces, thin silver films and nanoparticles.[224] The most significant increase in the Raman scattering (10^5-10^{10}-fold) was produced by aggregates of silver NP prepared by different methods.[33, 35, 225–228] The above enhancement in the intensity of spectral bands was illustrated by average values obtained based on a spectrum recorded for a large number of particles.[229] At the same time, ideal focusing of a light beam makes it possible to record SERS spectra from a tiny area of the NP contact. In this case, the experimentally observed enhancement of the Raman spectrum may approach 10^{15}. This enhancement is even sufficient for recording the Raman spectrum of several or even single molecule.[230–232]

Theoretical calculations of the surface plasmon electric field showed that the most intense fields and, hence, the highest enhancement factors of Raman scattering are reached near the areas with the highest surface curvature, whereas the lowest factors correspond to flat surfaces, which is consistent with the experiment. The electric field intensity rapidly decreases with distancing from the silver surface; hence, in the Raman spectra of not too large molecules, only bands corresponding to vibrations of groups located close to the surface are intensified rather than all bands.[233] The relative decrease in the electric field intensity with distancing from the metal surface is higher for surfaces with the higher curvature. For example, for silver nanowires with triangular and square cross-sections, the Raman scattering amplification factor decreased almost 1000-fold with distancing by 1 nm from the vertex of a 60° angle and only 100-fold at the same distance from a 90° angle (Fig. 19).[220]

For the same substance, relative intensities and the number of bands in a SERS or the Raman spectrum are as a rule different (Fig. 20).[226–235] One of the reasons for this consists in the fact that the adsorption and, especially, chemisorption [235, 236] change the molecule geometry. Moreover, according to the theory of SERS spectra, when a surface plasmon with a resonance frequency ω_0 is excited by incident electromagnetic

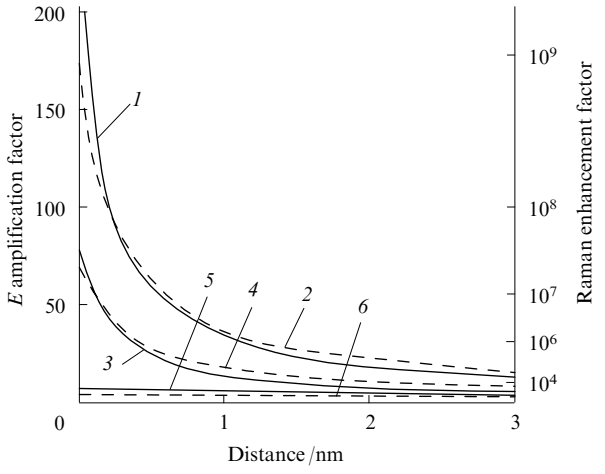


Figure 19. Dependences of the amplification factor of electric field intensity (E) and the Raman enhancement factor on the distance to the surface of silver nanowires with thickness of (*1*, *3*, *5*) 20 and (*2*, *4*, *6*) 50 nm and the following cross-sections: (*1*, *2*) triangle, (*3*, *4*) square, (*5*, *6*) circle.[220]
The distance was measured along the following directions: ▷---, ◇---, ○---.

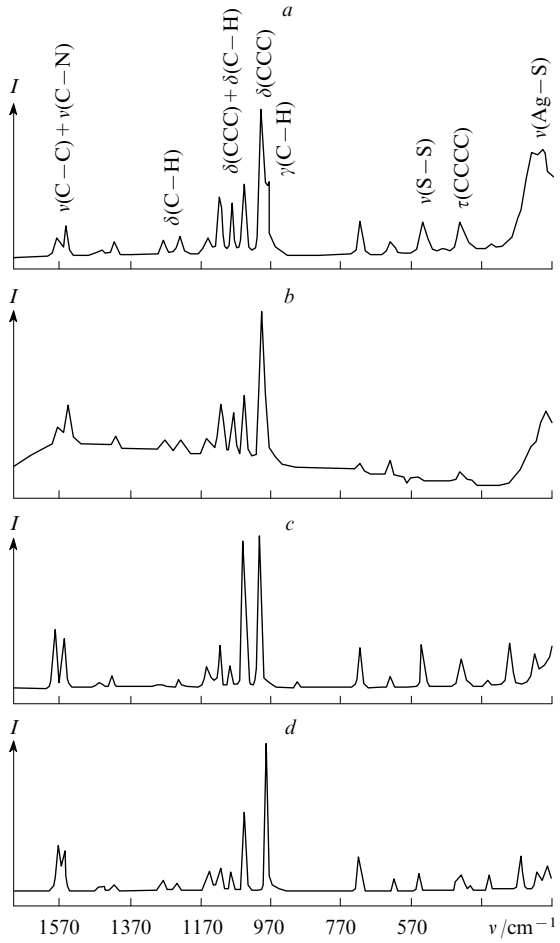


Figure 20. Raman spectra of bis(2-pyridyl) disulfide (bpds) measured under different conditions: (*a*) in aqueous solutions containing silver nanoparticles, (*b*) on a flat silver surface, (*c*) [Ag(bpds)]NO_3 complex and (*d*) pure bpds.[235]

radiation of the same frequency ω_0, the intensity of the Raman band with a shift ω is proportional to

$$E(\omega_0)^2 E(\omega + \omega_0)^2,$$

where $E(\omega)$ is the intensity of an electric field with frequency ω near the metal surface. If $\omega \ll \omega_0$, then $E(\omega + \omega_0) \approx E(\omega_0)$ and the intensity of the corresponding band in the Raman spectrum is proportional to $(\omega_0)^4$. As ω increases with the deviation of the electric field frequency from the resonance frequency ω_0, the value $E(\omega + \omega_0)$ quickly decreases. Hence, the coefficient of amplification of a Raman spectrum band should decrease with the increase in ω. In addition to this effect, the SERS spectra demonstrate anomalous intensities of individual bands and the appearance of the bands absent in the spectra of adsorbed or pure substances. To explain these phenomena, an additional mechanism was proposed [237] that attributes the near-surface enhancement of the Raman spectrum intensity to the electron transfer between the adsorbate and silver. This makes easier transitions between the ground and excited states of adsorbate molecules and results in amplification of the corresponding band. Almost immediately after the first SERS spectra were recorded for pyridine adsorbed on a silver electrode, this theory allowed the authors to explain the SERS dependence on the potential applied to the

electrode. The described mechanism is usually responsible for the $10-10^3$-fold increase in the intensity of SERS spectrum bands. The analysis of SERS spectra also requires that the intrinsic Raman spectra of silver NP be taken into account. The information on the latter can be found in a review. [238]

b. Peculiarities of fluorescence near the surface of silver nanoparticles

The near-surface increase in the electric field intensity observed upon excitation of the surface plasmon together with the enhancement of the Raman scattering described above lead to the increase in the intensity of fluorescence spectra (Fig. 21).

An increase in fluorescence of molecules adsorbed on the surface of silver NP or chemically bound to the NP was observed when the length of an SPR-related wave coincides with that of the fluorescence exciting wave.[239] This agrees with the fact that the experimental dependence of the fluorescence gain factor on the size of silver particles has a maximum in the coincidence of these wavelengthes.

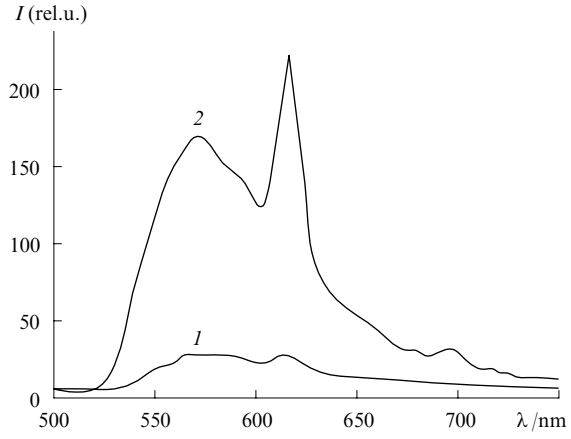


Figure 21. Fluorescence spectra of an $EuCl_3$ complex with tetracycline applied on (*1*) a glass support and (*2*) a support covered with a 30 nm-thick silver film.[231]

For molecules adsorbed on silver, the accelerated fluorescence decay is often observed.[240, 241] This phenomenon was associated with the interaction of a fluorescent molecule with a silver particle, which is particularly strong when a fluorophore is localised near the metal surface. The interaction of electronic levels of a silver particle with an adsorbate molecule makes easier the transition between the excited and ground states of a fluorescent molecule and shortens the excited state lifetime, which leads to the experimentally observed fast fluorescence decay, an increase in the quantum yield of the molecule excitation and an increase in the contribution of non-radiative processes in the excited state transitions.[240–243] When the exciting energy of a surface plasmon coincides with the energy of excited-to-ground transitions of the molecule, the excitation can be transferred to a silver NP, giving rise to its fluorescence. This phenomenon was experimentally observed for silver films [244, 245] and NP.[246] Fluorescence of silver NP in the presence of an adsorbate may be observed for low-power exciting radiation, whereas the intrinsic luminescence of NP in the range of 550–650 nm is manifested for powers of 30–100 W cm^{-1} (Ref. 247).

Shortening of the excited state lifetime favours an increase in the photostability of a fluorescent molecule, because it is the excited state that preferentially undergoes photochemical transitions.[248]

As compared with the Raman scattering intensity, the fluorescence intensity is proportional to the squared field intensity rather than to its fourth power. Together with the increase in the contribution of excited-state non-radiative transitions and the transfer of excitation to a silver particle, this causes the observed fluorescence gain for silver NP [239, 243] and films [244] that does not exceed 10^2-10^4. The higher gain factors (up to 10^8) were associated with two-photon excitation of fluorescence,[248] because in this case, the spectrum band intensity is proportional to the field intensity to the fourth power.

VI. Antibacterial properties of nanosilver

Antibacterial properties of metallic silver and its compounds are known from time immemorial. In small concentrations, silver is safe for human cells but lethal for the majority of bacteria and viruses and hence widely used in disinfection of water and food in everyday life and in the infection control in medicine.[249] To date, the unique antimicrobial and antiviral properties of silver compounds were comprehensively studied,[250–257] and this problem was the subject of several exhaustive reviews.[258–260] It seems improbable that microorganisms are capable of developing resistance to silver by mutations (except for the cases where the latter property existed *a priori*), because silver ions attack a vast number of various proteins in a cell. This valuable property became especially important today due to the increased number of species of pathogenic bacteria that are resistant to narrow-spectrum antibiotics and present a serious danger for human life and health.[261]

Bactericidal properties of metallic silver are associated with its slow oxidation and liberation of Ag^+ ions to the environment; hence, it seems promising to use nanosilver drugs as a special class of biocidal agents. Nanoparticles exhibit a high antibacterial effect due to their well-developed surface, which provides the maximum contact with the environment. Moreover, they are sufficiently small and capable of penetrating through cell membranes to affect intracellular processes from inside.

The effect of silver NP on the vital functions of gram-negative microorganisms *E. coli, V. cholera, P. aeruginosa* and *S. typhi* in their logarithmic growth stage was studied by modern high-precision methods.[262] For this purpose, solutions of silver NP with wide size distributions (from 3 to 25 nm) and different concentrations (0, 25, 50, 75, 100 μg ml^{-1}) were used. It was found that *V. cholera* and *P. aeruginosa* exhibited higher stability than *E. coli* and *S. typhi*; however, for the silver content of 75 μg ml^{-1}, the cessation of growth was observed for all microorganisms. The electron microscopic technique revealed that in addition to being fixed to the cell membrane, silver NP are capable of penetrating through it to be distributed inside a bacterium. This ability is inherent in separate NP rather than their agglomerates. Moreover, as a rule, the size of a membrane-bound NP does not exceed that of particles located inside the cell. Based on this fact, it was concluded that only clusters capable of interacting with the cell membrane are capable of incorporating into the cytoplasmic space.

Calculations of size distributions of NPs located inside a bacterium and fixed on its membrane have shown their diameter to be $\sim 5 \pm 2$ nm. Thus, this makes evident the assumption that bactericidal action of NP should strongly

depend on their size and increase as the latter decreases. Only NP with diameters smaller than 10 nm can directly interact with a bacterium. Under the assumption that all particles are spherical, the fraction of biologically active clusters in a given sample was calculated to be 0.093%. The growth of microorganisms was largely suppressed for $\sim$2000 of such clusters in average per cell. According to statistical studies, in the range of 1–10 nm, $\sim$98% of NP represented decahedra and icosahedra formed, as mentioned above, by tetrahedral clusters fused through their faces. It is well known that silver crystal facets {111}, which are abundant in these polyhedra, exhibit enhanced reactivity.[263–265] Moreover, a decrease in the NP size leads to an increase in the specific surface of a bactericidal specimen and, as a consequence, its total activity. This is probably the reason for the high biological activity of particles with diameters <10 nm.

The mechanism of NP penetration into a cell is not yet entirely clear. Strong changes in the membrane structure of the bacterium *E. coli*, an increase in its permeability and its ultimate death upon the interaction with NP were reported.[266] Observations of the membrane-bound and intracellular NP are important for understanding the bactericidal action of nanosilver. A bacterium wall contains a large amount of sulfur- and phosphorus-containing molecules that interact with an NP and loose their activity. Inside a bacterium, NP can interact with DNA; the latter thus looses its ability to replication,[266] which may lead to the cell death. Obviously, silver NP act as independent biocidal agents; nonetheless, to assess the contribution of silver ions to the NP activity, the concentration of Ag^+ ions was determined [262] to be several micromoles per litre. This points to a certain contribution of Ag^+ ions to the bactericidal properties of NP associated with insignificant dissolution of the latter. However, suppression of the bacterial growth under the action of silver nitrate demonstrated the differences in mechanisms of action of ions and NP on cells.

The same group of scientists studied the effect of silver NP on the activity of HIV-1.[267] For this purpose, NP samples stabilised by carbon foam, poly(*N*-vinyl-2-pyrrolidone) and bovine serum albumin were tested. In the first case, in the preliminary sonication step aimed at the preparation of an aqueous dispersion, the stabilising carbon-foam coating exfoliated to liberate NP with the non-modified silver surface. Figure 22 shows an image of HIV-1 with fixed silver NP, which was obtained in the dark-field mode by scanning TEM.[267]

Based on the results of scanning electron microscopy, two main conclusions were drawn. First, it turned out that in all experiments, NP fixed on the viral shell had the size from 1 to 10 nm. This confirms a conclusion on the clearly pronounced size dependence of biological activity of clusters.[262] Second, an ordered spatial distribution (as follows from the image) of NP was revealed, namely, NP bound to the viral shell were located at a distance of $\sim$28 nm from one another. These facts can be explained by taking into account the outer structure of an HIV-1 particle. Generally, its shell consists of a lipid membrane with incorporated glycoprotein centres that include trimers formed by two subunits, namely, surface glycoprotein gp120 and transmembrane glycoprotein gp41 with the internal matrix protein p17.[268] The main function of glycoprotein gp120 consists in recognition and binding of a viral particle to the host cell through the receptor region CD-4. It is well known that structure of gp120 subunit includes nine disulfide bonds of which three are localised in the immediate neighbourhood of the CD-4 receptor.[269] It is most probable that it is these fragments of glycoprotein gp120 localised at a distance of $\sim$22 nm from one another and including external disulfide

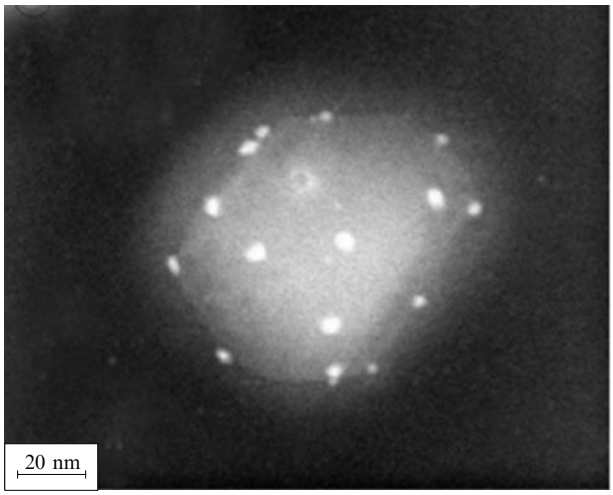


Figure 22. Scanning TEM image of HIV-1 with fixed silver NP recorded by the dark-field method.[267]

bonds that are the objects of the NP attack. Binding is thermodynamically disadvantageous for NP larger than the gp120 fragment ($\sim$14 nm [270]); the resulting bond is not strong. Despite the fact that the mechanism of the host cell initiation by HIV-1 is not entirely clear, it is evident that the CD-4 receptor of the gp120 fragment plays the key role in a stage of virus incorporation. Thus, the antiviral agent capable of selective interaction with this glycoprotein fragment suppresses the trend of HIV-1 to get bound to the cell and incorporate into it. Silver NP with non-modified surfaces exhibited the highest biological activity as such an agent. For all NP types taken in concentration of 25 μg ml^{-1}, the activity of HIV-1 virtually disappeared in the tests with cells MT-2 and cMAGI. However, in these tests, NP proved to be cytotoxic for studied cells themselves, which rules out their use. Probably, subsequent studies will be aimed at the modification of the surface properties and morphology of nanomaterials to make them capable of exerting highly selective effects on the chosen biological targets.

An answer was given [271] to a fundamental question of what physicochemical properties of silver NP surface are responsible for their strong antibacterial action. The sensitivity of nanosilver with respect to atmospheric oxygen was demonstrated long ago by Henglein.[15, 130] Species with oxidised surfaces bear chemisorbed Ag^+ ions. In experiments with *E. coli* strains (116S, J53), the effect of the silver NP surface state on their bactericidal activity was studied. [271] This included the preliminary synthesis of silver NP (9.2 ± 2.8 nm) by the reduction with $NaBH_4$. A partially oxidised material with adsorbed Ag^+ ions was obtained by flowing O_2 through a NP solution for 30 min. A mass spectrometric study has shown that the equilibrium content of free silver ions in the NP solution did not exceed 0.1% of the total amount of metal, which makes virtually no contribution to the biocidal activity. It was found that the minimum concentration of oxidised NP capable of complete inhibition of growth of *E. coli* 116S and J53 (in the logarithmic phase) was merely 2 nmol $litre^{-1}$, which corresponds to the metal content of 5.4 μg ml^{-1}. Nanosilver synthesised by the reduction in an inert atmosphere exhibited no antibacterial activity; the latter was also lost by oxidised nanoparticles after their treatment with sodium borohydride. Based on spectral data and using an equation [15]

$$\lambda = \lambda_0 \left(1 + \frac{[Ag^+]}{[Ag]}\right)^{1/2},$$

where λ_0 and λ are the absorption maxima before and after oxidation, respectively, and $[Ag^+]$ and [Ag] are the concentration of adsorbed ions and the overall concentration of the metal in solution, respectively, which was derived under an assumption that $[Ag^+] \ll [Ag]$, the content of adsorbed Ag^+ ions was assessed to be ~12% of the total silver amount. Thus, presumably, the key contribution to the antibacterial activity of silver NP was made by Ag^+ ions adsorbed on the NP surface rather than by neutral metal atoms. To elucidate the effect of the size of oxidised NP on the bactericidal action of their dispersions, coarse (62 ± 18 nm) silver NP were synthesised. It was found that for the same metal content in dispersions, the biological activity exhibited by NP with the average diameter of 9.8 nm was 10 times higher than that of coarse silver clusters. The data on the bactericidal activity of coarse NP clusters (from 25 nm and larger) can be found in Ref. 53. Studies on the effect of NP on bacterial cultures stable against silver nitrate [*E. coli* mutants, namely, strains 116$AgNO_3$R and J53(pMG101)] have shown that these microorganisms retain ability for reproduction at the highest NP concentrations attainable under experimental conditions. This fact indirectly suggests that chemisorbed ions exert the key effect on the biocidal properties of particles. Detailed information of silver-resistant bacteria can be found in reviews [258, 259] and original papers.[160, 272, 273].

Discoveries of the past decade demonstrated that optical, catalytic and other properties of nanosized objects strongly depend on their geometry;[274] however, when the present review was in the stage of preparation, only one publication [275] was available that dealt with the dependence of antibacterial properties of silver NP on their morphology. To elucidate these relationships, the effect of solutions of silver nitrate, spherical NP, nanorods and truncated triangles with the same concentration with respect to metal (1, 6, 12, 12.5, 50 and 100 μg per 100 ml of nutrient medium) on the *E. coli* ATCC 10536 cell culture was studied. It was shown that truncated triangles virtually entirely inhibited the microorganism growth starting from the total silver content of 1 μg; spherical NP substantially suppressed the reproduction at 12.5 μg and completely stopped it at 50–100 μg. For nanorods, the continued growth of separate colonies was observed even for the silver content of 100 μg. The biocidal activity of silver nitrate turned out to be comparable with that of spherical NP. The different biological action of clusters with different shapes was probably associated with the different contribution of the most active {111} faces in the overall surface of particles. Thus for truncated nanotriangles, the contribution of these faces into the surface structure is the maximum, whereas nanorods contain them only on their ends. In spherical and quasi-spherical particles, the contribution of {111} faces in the surface structure is also small. Further studies in this field should be aimed at the quantitative assessment of the effect of different surfaces on the bactericidal capacity and activity of NP and at the elucidation of mechanisms of injuries of bacterial cells.

At present, the fundamental studies of mechanisms of antibacterial action of silver NP are still in their infancy. Nonetheless, the number of publications devoted to the use of bactericidal properties of silver nanoparticles in solving the applied problems of medicine and industry progressively increases. For example, a positive synergistic effect of nano-silver and different antibiotics in the control over *S. aureus* and *E. coli* was reported.[276] A simple and cheap procedure of the formation of a biocompatible polyelectrolyte layer based on an amidated poly(ethylene terephthalate) film containing silver clusters and exhibiting high anticoagulation and bactericidal activity was described.[277] Presumably, such films may have potential applications in the surface modification of different medicinal devices, particularly, cardiovascular implants. The preparation and properties of food packing materials based on biodegradable natural polymers that exhibit antibacterial properties due to the presence of silver-containing nanocomposites were described.[278] A large number of studies were devoted to impregnation of textiles with solutions of silver NP to provide them with antibacterial properties.[279–281] A simple and effective industrial procedure of impregnation of textiles and non-woven fibres with silver nanoparticles (~2–3 nm) was developed.[282] It was shown that after the impregnation of fibres with 2×10^{-5}% NP solution, their overall bacteriostatic activity with respect to gram-positive microorganism *S. aureus* ATCC 6538 and gram-negative microorganism *E. coli* ATCC 25922 did not disappear even after ten procedures of wet treatment with the use of detergents. Moreover, tests of this item on animals demonstrated its total safety for skin.

VII. Conclusion

The above analysis of the literature data revealed no decay in the activity of studies devoted to the synthesis of silver NP, despite the fact that the general principles of preparative NP syntheses are already sufficiently well developed. However, the problems of synthesis of hydrophilic silver NP with aggregative stability in a wide pH range and their reproducible preparation are yet far from being completely solved. At the same time, hydrophilicity turns out to be a valuable property for the practical use of NP in analytical chemistry, biology and medicine, because almost all objects studied required the presence of aqueous medium. At present, the development of versatile and highly effective methods for purification of silver NP dispersions is an independent and challenging problem. This is necessary for their further use in microelectronics, medicine, spectroscopy, catalysis and other fields.

The number of studies devoted to the use of silver NP and aimed at the enhancement of the Raman and fluorescence spectra of different organic molecules increases every year. It is the use of silver NP, which exhibit the highest SPR excitation efficiency among all known conductors, that made it possible to record the Raman spectrum of a single molecule.[230, 231] This may later lead to the development of ultrasensitive analytical methods, *e.g.*, for the detection of superecotoxicants. The possibility of tuning the SPR frequency by varying the NP size and shape is very important for the mentioned applications of NP. The low energy losses in the excitation of a surface plasmon make it possible to design miniature waveguides based on silver nanorods, nanowires and systems of ordered NP for the transfer of optical oscillations in nanodevices.[213–215] Silver nanoparticles of different shapes and their ordered associates may form the basis for the development of new directions of physical non-linear optics associated with designing materials with unique optical characteristics and a wide application spectrum.

Today, the fact that silver NP exhibit high activity with respect to all biological objects from viral species to human organism is beyond question. The fact that the number of studies devoted to antiviral and antibacterial activity of silver NP increases every year confirms the high interest in both

fundamental and applied aspects of this problem. At the same time, studies aimed at the quantitative assessment of the biological action of silver NP on humans and animals are practically absent. Unfortunately, it is true that under certain conditions, many NP types (silver NP too, albeit probably to a lesser extent) can exert an extremely negative effect on living systems and even cause severe and irreversible changes in an organism. In this context, it is not surprising that a new field of medicine, nanotoxicology, is emerging nowadays, aimed at the development of complex approaches to studying the biological (including toxicological) activity of NP as a function of their composition, size, shape and functional surface coverage.[283–285] In future, these studies may lead to the development of highly effective and low-toxic medicinal drugs with a broad spectrum of applications, based on silver NP.

This review was prepared with the financial support by the Federal Target Programme 'Studies and Developments on High-Priority Directions of the Development of the Research and Technological Complex in 2007 – 2012' (Project No. 2007-3-2.3-07-06-007).

References

1. D J Barber, I C Freestone *Archaeometry* **32** 33 (1990)
2. J A Creighton, C G Blatchford, M G Albrecht *J. Chem. Soc., Faraday Trans.* **75** 790 (1979)
3. P C Lee, D Meisel *J. Phys. Chem.* **86** 3391 (1982)
4. A Henglein *Chem. Rev.* **89** 1861 (1989)
5. T A Taton, C A Mirkin, R L Letsinger *Science* **289** 1757 (2000)
6. Y C Cao, R Jin, C A Mirkin *Science* **297** 1536 (2002)
7. J Zhang, J Malicka, I Gryczynski, J R Lakowicz *J. Phys. Chem. B* **109** 7643 (2005)
8. G K Vertelov, A Yu Olenin, G V Lisichkin *Zh. Anal. Khim.* **62** 903 (2007) [a]
9. A Yu Olenin, Yu A Krutyakov, A A Kudrinskiy, G V Lisichkin *Kolloid. Zh.* **70** 78 (2008) [b]
10. J Turkevich, P C Stevenson, J Hiller *Discuss. Faraday Soc.* (11) 55 (1951)
11. G Schmid *Chem. Rev.* **92** 1709 (1992)
12. R Jin, Y W Cao, C A Mirkin, K L Kelly, G S Schatz, J G Zheng *Science* **294** 1901 (2001)
13. G N R Tripathi, M Clements *J. Phys. Chem. B* **107** 11125 (2003)
14. A Henglein, M Giersig *J. Phys. Chem. B* **103** 9533 (1999)
15. A Henglein *Chem. Mater.* **10** 444 (1998)
16. B G Ershov, E Janata, A Henglein *J. Phys. Chem.* **97** 339 (1993)
17. Y Xiong, I Washio, J Chen, M Sadilek, Y Xia *Angew. Chem., Int. Ed.* **46** 4917 (2007)
18. A Henglein *J. Phys. Chem.* **83** 2209 (1979)
19. D Meisel *J. Am. Chem. Soc.* **101** 6133 (1979)
20. A Henglein *J. Phys. Chem.* **84** 3461 (1980)
21. A Henglein, J Lilie *J. Am. Chem. Soc.* **103** 1059 (1981)
22. Z S Pillai, P V Kamat *J. Phys. Chem. B* **108** 945 (2004)
23. D D Evanoff Jr, G Chumanov *ChemPhysChem* **6** 1221 (2005)
24. V K LaMer, R H Dinegar *J. Am. Chem. Soc.* **72** 4847 (1950)
25. J-L Look, G H Bogush, C F Zukoski *Faraday Discuss. Chem. Soc.* 345 (1990)
26. S Kim, C Zukoski *J. Colloid Interface Sci.* **139** 198 (1990)
27. D L Van Hyning, C F Zukoski *Langmuir* **14** 7034 (1998)
28. D L Van Hyning, W G Klemperer, C F Zukoski *Langmuir* **17** 3120 (2001)
29. D L Van Hyning, W G Klemperer, C F Zukoski *Langmuir* **17** 3128 (2001)
30. S P Gubin, N A Kataeva *Koord. Khim.* **32** 883 (2006) [c]
31. T Yonezawa, S Onoue, N Kimizuka *Langmuir* **16** 5218 (2000)
32. R C Doty, T R Tshikhudo, M Brust, D G Fernig *Chem. Mater.* **17** 4630 (2005)
33. X Zou, H Bao, H Guo, L Zhang, L Qi, J Jiang, L Niu, S Dong *J. Colloid Interface Sci.* **295** 401 (2006)
34. S Zhao, K Zhang, J An, Y Sun, C Sun *Mater. Lett.* **60** 1215 (2006)
35. S Zhao, K Zhang, Y Sun, C Sun *Bioelectrochemistry* **69** 10 (2006)
36. X Li, J Zhang, W Xu, H Jia, X Wang, B Yang, B Zhao, B Li, Y Ozaki *Langmuir* **19** 4285 (2003)
37. J Liu, J-B Lee, D-H Kim, Y Kim *Colloids Surf., A* **302** 276 (2007)
38. M Brust, M Walker, D J Schiffrin, R Whyman *J. Chem. Soc., Chem. Commun.* 801 (1994)
39. N Sandhyarani, M R Resmi, R Unnikrishnan, K Vidyasagar, S Ma, M P Antony, G P Selvam, V Visalakshi, N Chandrakumar, K Pandian, Y-T Tao, T Pradeep *Chem. Mater.* **12** 104 (2000)
40. S He, J Yao, S Xie, S Pang, H Gao *Chem. Phys. Lett.* **343** 28 (2001)
41. C J Kiely, J Fink, J G Zheng, M Brust, D Bethell, D J Schiffrin *Adv. Mater.* **12** 640 (2000)
42. R M Lahtinen, S F L Mertens, E East, C J Kiely, D J Schiffrin *Langmuir* **20** 3289 (2004)
43. M Husein, E Rodil, J Vera *Langmuir* **19** 8467 (2003)
44. P Mulvaney *Langmuir* **12** 788 (1996)
45. A Manna, T Imae, M Iida, N Hisamatsu *Langmuir* **17** 6000 (2001)
46. C A Waters, A J Mills, K A Johnson, D J Schiffrin *Chem. Commun.* 540 (2003)
47. K J Lee, Y-I Lee, I-K Shim, J Joung, Y S Oh *J. Colloid Interface Sci.* **304** 92 (2006)
48. W Cheng, E Wang *J. Phys. Chem. B* **108** 24 (2004)
49. Y Yang, S Liu, K Kimura *Colloids Surf., A* **290** 143 (2006)
50. Y Yin, Z-Y Li, Z Zhong, B Gates, Y Xia, S Venkateswaran *J. Mater. Chem.* **12** 522 (2002)
51. S Panigrahi, S Kundu, S K Ghosh, S Nath, T Pal *J. Nanopart. Res.* **6** 411 (2004)
52. L Qu, L Dai *J. Phys. Chem. B* **109** 13985 (2005)
53. A Panàček, L Kvítek, R Prucek, M Kolář, R Večeřová, N Pizúrová, V K Sharma, T Nevěčná, R Zbořil *J. Phys. Chem. B* **110** 16248 (2006)
54. L-C Steve Hsu, R-T Wu *Mater. Lett.* **61** 3719 (2007)
55. S P Chandran, M Chaudhary, R Pasricha, A Ahmad, M Sastry *Biotechnol. Prog.* **22** 577 (2006)
56. S S Shankar, A Ahmad, M Sastry *Biotechnol. Prog.* **19** 1627 (2003)
57. X Wang, J Zhuang, Q Peng, Y Li *Nature (London)* **437** 121 (2005)
58. P -Y Silvert, R Herrera-Urbina, N Duvauchelle, V Vijayakrishnan, K J Tekaia-Elhissen *J. Mater. Chem.* **6** 573 (1996)
59. Y Sun, Y Xia *Science* **298** 2176 (2002)
60. Z Chen, L Gao *Mater. Res. Bull.* **42** 1657 (2007)
61. I Pastoriza-Santos, L M Liz-Marzán *Pure Appl. Chem.* **72** 83 (2000)
62. M Green, N Allsop, G Wakefield, P J Dobson, J L Hutchison *J. Mater. Chem.* **12** 2671 (2002)
63. S W Kim, J Paark, Y Jang, Y Chung, S Hwang, T Hyeon *Nano Lett.* **3** 1289 (2003)
64. S D Bunge, T J Boyle, T J Headley *Nano Lett.* **3** 901 (2003)
65. M Boutonnet, J Kizling, P Stenius *Colloids Surf., A* **5** 209 (1982)
66. K Kurihara, J Kizling, P Stenius, J H Fendler *J. Am. Chem. Soc.* **105** 2574 (1983)
67. I Ravet, J B Nagy, E G Derouane *Stud. Surf. Sci. Catal.* **31** 505 (1987)
68. K Osseo-Asare, F Arriagada *Ceram. Trans.* **12** 3 (1990)
69. T F Towey, A Khan-Lodhi, B H Robinson *J. Chem. Soc., Faraday Trans.* **86** 3757 (1990)
70. T Hirai, H Sato, I Komasawa *Ind. Eng. Chem. Res.* **32** 3014 (1993)
71. M A López-Quintela, J Rivas *J. Colloid Interface Sci.* **158** 446 (1993)
72. R Bandoyopadhyaya, R Kumar, K S Gandhi *Langmuir* **13** 3610 (1997)

73. J Schmidt, C Guesdon, R Schomäcker *J. Nanopart. Res.* **1** 267 (1999)
74. P Barnickel, A Wokaun *Mol. Phys.* **69** 1 (1990)
75. P Barnickel, A Wokaun, W Sager, H F Eicke *J. Colloid Interface Sci.* **148** 80 (1992)
76. M P Pileni, T Zemb, C Petit *Chem. Phys. Lett.,* **118** 414 (1985)
77. J H Fendler *Chem. Rev.* **87** 877 (1987)
78. C Petit, P Lixon, M P Pileni *J. Phys. Chem.* **97** 12974 (1993)
79. A Taleb, C Petit, M P Pileni *Chem. Mater.* **9** 950 (1997)
80. M Sastry *Curr. Sci.* **85** 1735 (2003)
81. K S Mayya, F Caruso *Langmuir* **19** 6987 (2003)
82. Y Negishi, T Tsukuda *J. Am. Chem. Soc.* **125** 4046 (2003)
83. A C Templeton, M J Hosteler, E K Warmoth, S Chen, C M Hartshorn, V M Krishnamurthy, M D E Forbes, R W Murray *J. Am. Chem. Soc.* **120** 4845 (1998)
84. A Swami, A Kumar, M Sastry *Langmuir* **19** 1168 (2003)
85. T Pellegrino, L Manna, S Kudera, T Liedl, D Koktysh, A L Rogach, S Keller, J Radler, G Natile, W J Parak *Nano Lett.* **4** 703 (2004)
86. Y Wang, J F Wong, X Teng, X Z Lin, H Yang *Nano Lett.* **3** 1555 (2003)
87. B L V Prasad, S K Arumugam, T Bala, M Sastry *Langmuir* **21** 822 (2005)
88. W Wang, S Efrima, O Regev *Langmuir* **14** 602 (1998)
89. W Wang, X Chen, S Efrima *J. Phys. Chem. B* **103** 7238 (1999)
90. S K Ghosh, S Kundu, M Mandal, S Nath, T Pal *J. Nanopart. Res.* **5** 577 (2003)
91. P V Kamat, M Flumiani, G V Hartland *J. Phys. Chem. B* **102** 3123 (1998)
92. J Xu, X Han, H Liu, Y Hu *Colloids Surf., A* **273** 179 (2006)
93. R Zana *Adv. Colloid Interface Sci.* **97** 203 (2002)
94. D Kitamoto, H Isoda, T Nakahara *J. Biosci. Bioeng.* **94** 187 (2002)
95. Y W Xie, Y Li, R Q Ye *J. Disp. Sci. Technol.* **26** 455 (2005)
96. Y Xie, R Ye, H Liu *Colloids Surf., A* **279** 175 (2006)
97. J R Heath, C M Knobler, D V Leff *J. Phys. Chem. B* **101** 189 (1997)
98. A Swami, P R Selvakannan, R Pasricha, M Sastry *J. Phys. Chem. B* **108** 19269 (2004)
99. L Zhang, Y Shen, A Xie, S Li, B Jin, Q Zhang *J. Phys. Chem. B* **110** 6615 (2006)
100. I Lisiecki, M P Pileni *J. Phys. Chem.* **99** 5077 (1995)
101. R P Bagwe, K C Khilar *Langmuir* **13** 6432 (1997)
102. R P Bagwe, K C Khilar *Langmuir* **16** 905 (2000)
103. D W Matson, J L Fulton, R D Smith *Mater. Lett.* **6** 31 (1987)
104. J P Cason, K Khambaswadkar, C B Roberts *Ind. Eng. Chem. Res.* **39** 4749 (2000)
105. J P Cason, C B Roberts *J. Phys. Chem. B* **104** 1217 (2000)
106. K P Johnston, K L Harrison, M J Clarke, S M Howdle, M P Heitz, F V Bright, C Carlier, T W Randolph *Science* **271** 624 (1996)
107. Z-T Liu, C Erkey *Langmuir* **17** 274 (2001)
108. R G Zielinski, N Rosov, E W Kaler, S R Kline *Langmuir* **13** 3934 (1997)
109. G B Jacobson, C T Lee, K P Johnston *J. Org. Chem.* **64** 1201 (1999)
110. M Ji, X Chen, C M Wai, J L Fulton *J. Am. Chem. Soc.* **121** 2631 (1999)
111. Y-P Sun, P Atorngitjawat, M J Meziani *Langmuir* **17** 5707 (2001)
112. H Ohde, F Hunt, C M Wai *Chem. Mater.* **13** 4130 (2001)
113. P S Shah, J D Holmes, R C Doty, K P Johnston, B A Korgel *J. Am. Chem. Soc.* **122** 4245 (2000)
114. A Kameo, T Yoshimura, K Esumi *Colloids Surf., A* **215** 181 (2003)
115. M C McLeod, R S McHenry, E J Beckman, C B Roberts *J. Phys. Chem. B* **107** 2693 (2003)
116. A Henglein, R Tausch-Treml *J. Colloid Interface Sci.* **80** 84 (1981)
117. B G Ershov, A Henglein *J. Phys. Chem. B* **102** 10663 (1998)
118. B G Ershov, A Henglein *J. Phys. Chem. B* **102** 10667 (1998)
119. A Pyatenco, K Shimokawa, M Yamagichi, O Nishimiura, M Suzuki *Appl. Phys. A* **79** 803 (2004)
120. A V Simakin, V V Voronov, N A Kirichenko, G A Shafeev *Appl. Phys. A* **79** 1127 (2004)
121. R A Ganeev, M Baba, A I Ryasnyansky, M Suzuki, H Kuroda *Opt. Commun.* **240** 437 (2004)
122. T Tsuji, T Kakita, M Tsuji *Appl. Surf. Sci.* **206** 314 (2003)
123. G A Shafeev, E Freysz, F Bozon-Verduraz *Appl. Phys. A* **78** 307 (2004)
124. Y Chen, C Yeh *Colloids Surf., A* **197** 133 (2002)
125. V Amendola, S Polizzi, M Meneghetti *Langmuir* **23** 6766 (2007)
126. W T Nichols, G Malyavanatham, D E Henneke, J R Brock, M F Becker, J W Keto, H D Glicksman *J. Nanopart. Res.* **2** 141 (2000)
127. W T Nichols, J W Keto, D E Henneke, J R Brock, G Malyavanatham, M F Becker, H D Glicksman *Appl. Phys. Lett.* **78** 1128 (2001)
128. J Lee, M F Becker, J W Keto *J. Appl. Phys.* **89** 8146 (2001)
129. F Mafuné, J Kohno, Y Takeda, T Kondow, H Sawbe *J. Phys. Chem. B* **104** 9111 (2000)
130. A Henglein *J. Phys. Chem.* **97** 5457 (1993)
131. E Janata, A Henglein, B G Ershov *J. Phys. Chem.* **98** 10888 (1994)
132. X Xu, Y Yin, X Ge, H Wu, Z Zhang *Mater. Lett.* **37** 354 (1998)
133. Y J Zhu, Y Qian, X Li, M Zhang *Chem. Commun.* 1081 (1997)
134. S-H Choi, S-H Lee, Y-M Hwang, K-P Lee, H-D Kang *Radiat. Phys. Chem.* **67** 517 (2003)
135. J A Jacob, S Kapoor, N Biswas, T Mukherjee *Colloids Surf., A* **301** 329 (2007)
136. B Soroushian, I Lampre, J Belloni, M Mostafavi *Radiat. Phys. Chem.* **72** 111 (2005)
137. J F Hund, M F Bertino, G Zhang, C Sotiriou-Leventis, N Leventis, A T Tokuhiro, J Farmer *J. Phys. Chem. B* **107** 465 (2003)
138. D Lawless, S Kapoor, P Kennepohl, D Miesel, N Serpone *J. Phys. Chem.* **98** 9619 (1994)
139. A Sarkany, I Sajo, P Hargittai, Z Papp, E Tombacz *Appl. Catal., A* **293** 41 (2005)
140. S P Ramnani, J Biswal, S Sabharwal *Radiat. Phys. Chem.* **76** 1290 (2007)
141. P Chen, L Song, Y Liu, Y Fang *Radiat. Phys. Chem.* **76** 1165 (2007)
142. M P Andrews, G A Ozin *Chem. Mater.* **1** 174 (1989)
143. G A Ozin, H Huber, S A Mitchell *Inorg. Chem.* **18** 2932 (1979)
144. M P Andrews, G A Ozin *J. Phys. Chem.* **90** 2922 (1986)
145. S A Mitchell, G A Kenney-Wallace, G A Ozin *J. Am. Chem. Soc.* **103** 6030 (1981)
146. H Huber, P Mackenzie, G A Ozin *J. Am. Chem. Soc.* **102** 1548 (1980)
147. Yu A Novozhilov, M A Lunina *Zh. Fiz. Khim.* **42** 2114 (1968) [d]
148. G Bredig. *Z. Electrochem.* **4** 514 (1898)
149. T Svedberg *Kolloidn. Z.* **21** 1 (1919)
150. M Moskovits, G Ozin *Cryochemistry* (New York: Wiley, 976)
151. *Chemistry and Physics of Matrix Isolated Species* (Eds L Andrews, M Moskovits) (Amsterdam: North Holland, 1989)
152. K J Klabunde *Chemistry of Free Atoms and Particles* (New York: Academic Press, 1980)
153. S E Kondakov, A Yu Olenin, V V Smirnov *Bull. Soc. Chim. Belg.* **104** 369 (1995)
154. A Yu Vasil'kov, A Yu Olenin, E F Titova, V A Sergeev *J. Colloid Interface Sci.* **169** 356 (1995)
155. M A Lunina, Yu A Novozhilov *Kolloid. Zh.* **31** 467 (1969) [b]
156. M A Lunina, Doctoral Thesis in Chemical Sciences, Moscow Chemical and Technological Institute, Moscow, 1970
157. D P E Dickson *J. Magn. Magn. Mater.* **203** 46 (1999)
158. S Mann *Nature (London)* **365** 499 (1993)
159. S Oliver, A Kupermann, N Coombs, A Lough, G A Ozin *Nature (London)* **378** 47 (1995)
160. P Messner, D Pum, M Sara *Angew. Chem., Int. Ed.* **38** 1034 (1999)

161. J R Stephen, S J Macnaughton *Curr. Opin. Biotechnol.* **10** 230 (1999)
162. T Klaus, R Joerger, E Olsson, C G Granqvist *Proc. Natl. Acad. Sci. USA* **96** 13611 (1999)
163. T Klaus-Joerger, R Joerger, E Olsson, C G Granqvist *Trends Biotechnol.* **19** 15 (2001)
164. P Mukherjee, A Ahmad, D Mandal, S Senapati, S R Sainkar, M I Khan, R Parishcha, P V Ajaykumar, M Alam, R Kumar, M Sastry *Nano Lett.* **1** 515 (2001)
165. C T Dameron, R N Reese, R K Mehra, P J Kortan, M L Carrol, M L Steigerwald, L E Brus, D R Winge *Nature (London)* **338** 596 (1989)
166. M C Brelle, J Z Zhang, L Nguyen, R K Mehra *J. Phys. Chem. A* **103** 10194 (1999)
167. A Ahmad, P Mukherjee, S Senapati, D Mandal, M I Khan, R Kumar, M Sastry *Colloids Surf., B* **28** 313 (2003)
168. N Durán, P D Marcato, O L Alves, G I H De Souza, E Esposito *J. Nanobiotechnol.* **3**:**8** 1 (2005)
169. D K Newman, R Kolter *Nature (London)* **405** 94 (2000)
170. S A Kumar, M K Abyaneh, S W Gosavi, S K Kulkarni, R Pasricha, A Ahmad, M I Khan *Biotechnol. Lett.* **29** 439 (2007)
171. M Kowshik, S Ashtaputre, S Kharrazi, W Vogel, J Urban, S K Kulkarni, K M Paknikar *Nanotechnology* **14** 95 (2003)
172. J T Trevors *Enzyme Microb. Technol.* **9** 331 (1987)
173. R R Naik, S J Stringer, G Agarwal, S E Jones, M O Stone *Nature Mater.* **1** 169 (2002)
174. R R Naik, L L Brott, S J Clarson, M O Stone *J. Nanosci. Nanotechnol.* **2** 95 (2002)
175. S-W Lee, C Mao, C E Flynn, A M Belcher *Science* **296** 892 (2002)
176. S R Whaley, D S English, E L Hu, P F Barbara, A M Belcher *Nature (London)* **405** 665 (2000)
177. Z R Ul'berg, N V Pertsov, Yu F Bazhenov, L G Marochko *Kolloid. Zh.* **50** 1026 (1988) [b]
178. Z R Ul'berg, V I Karamushka, T G Gruzina *Biotekhnologiya* **1** 109 (1986)
179. Z R Ul'berg, V I Karamushka, A S Dukhin, F D Ovcharenko *Dokl. Akad. Nauk SSSR* **303** 738 (1988) [e]
180. D O Yener, J Sindel, C A Randall, J H Adair *Langmuir* **18** 8692 (2002)
181. L Huang, H Wang, Z Wang, A Mitra, K N Bozhilov, Y Yan *Adv. Mater.* **14** 61 (2002)
182. D Yu, V W-W Yam *J. Am. Chem. Soc.* **126** 13200 (2004)
183. G Wei, H Zhou, Z Liu, Y Song, L Wang, L Sun, Z Li *J. Phys. Chem. B* **109** 8738 (2005)
184. S-H Zhang, Z-X Xie, Z-Y Jiang, X Xu, J Xiang, R-B Huang, L-S Zheng *Chem. Commun.* 1106 (2004)
185. A Drury, S Chaure, M Kröll, V Nicolosi, N Chaure, W J Blau *Chem. Mater.* **19** 4252 (2007)
186. Y Sun, Y Yin, B T Mayers, T Herricks, Y Xia *Chem. Mater.* **14** 4736 (2002)
187. J Bai, Y Qin, C Jiang, L Qi *Chem. Mater.* **19** 3367 (2007)
188. N R Jana, L Gearheart, C J Murphy *Chem. Commun.* 617 (2001)
189. B Wiley, Y Sun, B Mayers, Y Xia *Chem. – Eur. J.* **11** 454 (2005)
190. C J Murphy, A M Gole, S E Hunyadi, C J Orendorff *Inorg. Chem.* **45** 7544 (2006)
191. S Ino, D Ogawa *J. Phys. Soc. Jpn.* **22** 1365 (1967)
192. S Ino *J. Phys. Soc. Jpn.* **21** 346 (1966)
193. L D Marks *Rep. Prog. Phys.* **57** 603 (1994)
194. Y Sun, B Gates, B Mayers, Y Xia *Nano Lett.* **2** 165 (2002)
195. Y Sun, Y Xia *Adv. Mater.* **14** 833 (2002)
196. D M Ledwith, A M Whelan, J M Kelly *J. Mater. Chem.* **17** 2459 (2007)
197. X Zou, E Ying, H Chen, S Dong *Colloids Surf., A* **303** 226 (2007)
198. S Chen, Z Fan, D L Carroll *J. Phys. Chem. B* **106** 10777 (2002)
199. Y Xiong, I Washio, J Chen, H Cai, Z-Y Li, Y Xia *Langmuir* **22** 8563 (2006)
200. Y Sun, B Mayers, Y Xia *Nano Lett.* **3** 675 (2003)
201. P V Kamat *J. Phys. Chem. B* **106** 7729 (2002)
202. A K Popov, R S Tanke, J Brummer, G Taft, M Loth, R Langlois, A Wruck, R Schmitz *Nanotechnology* **17** 1901 (2006)
203. D J Campbell, Y Xia *J. Chem. Educ.* **84** 91 (2007)
204. L M Liz-Marzán *Mater. Today* **7** 26 (2004)
205. A Moores, F Goettmann *New J. Chem.* **30** 1121 (2006)
206. L J Sherry, S-H Chang, G C Schatz, R P Van Duyne *Nano Lett.* **5** 2034 (2005)
207. H Mertens, J Verhoeven, A Polman, F D Tichelaar *Appl. Phys. Lett.* **85** 1317 (2004)
208. J Tiggesbaumker, L Koller, H O Lutz, K H Meiwesbroer *Chem. Phys. Lett.* **190** 42 (1992)
209. A Liebsch *Phys. Rev. B* **48** 11317 (1993)
210. Y Hosoya, T Suga, T Yanagawa, Y Kurokawa *J. Appl. Phys.* **81** 1475 (1997)
211. W Cai, H Hofmeister, T Rainer, W Chen *J. Nanopart. Res.* **3** 443 (2001)
212. P Billaud, J-R Huntzinger, E Cottancin, J Lermé, M Pellarin, L Arnaud, M Broyer, N Del Fatti, F Vallée *Eur. Phys. J., D* **43** 271 (2007)
213. A W Sanders, D A Routenberg, B J Wiley, Y Xia, E R Dufresne, M A Reed *Nano Lett.* **6** 1822 (2006)
214. S A Maier, M L Brongersma, P G Kik, S Meltzer, A A G Requicha, H A Atwater *Adv. Mater.* **13** 1501 (2001)
215. A L Stepanov, J R Krenn, H Ditlbacher, A Hohenau, A Drezet, B Steinberger, A Leitner, F R Aussenegg *Opt. Lett.* **30** 1524 (2005)
216. T Jensen, L Kelly, A Lazarides, G C Schatz *J. Clust. Sci.* **10** 295 (1999)
217. B J Wiley, S H Im, Z-Y Li, J McLellan, A Siekkinen, Y Xia *J. Phys. Chem. B* **110** 15666 (2006)
218. J J Mock, M Barbic, D R Smith, D A Schultz, S Schultz *J. Chem. Phys.* **116** 6755 (2002)
219. J Nelayah, M Kociak, O Stéphan, F J G De Abajo, M Tencé, L Henrard, D Taverna, I Pastoriza-Santos, L M Liz-Marzán, C Colliex *Nature Phys.* **3** 348 (2007)
220. J P Kottmann, O J F Martin, D R Smith, S Schultz *Phys. Rev. B* **64** 235402 (2001)
221. R Jin, Y C Cao, E Hao, G S Métraux, G C Schatz, C A Mirkin *Nature (London)* **425** 487 (2003)
222. M Fleischmann, P J Hendra, A J McQuillan *Chem. Phys. Lett.* **26** 163 (1974)
223. A J McQuillan, P J Hendra, M Fleischmann *J. Electroanal. Chem.* **65** 933 (1975)
224. A Campion, P Kambhampati *Chem. Soc. Rev.* **27** 241 (1998)
225. I Khan, D Cunningham, R E Littleford, D Graham, W E Smith, D W McComb *Anal. Chem.* **78** 224 (2006)
226. A Tao, F Kim, C Hess, J Goldberger, R He, Y Sun, Y Xia, P Yang *Nano Lett.* **3** 1229 (2003)
227. J B Jackson, N J Halas *Proc. Natl. Acad. Sci. USA* **101** 17930 (2004)
228. B Fang, Y Gao, M Li, G Wang, Y Li *Microchim. Acta* **147** 81 (2004)
229. G H Gu, J Kim, L Kim, J S Suh *J. Phys. Chem. C* **111** 7906 (2007)
230. S R Emory, S Nie *Science* **275** 1102 (1997)
231. K Kniepp, Y Wang, H Kneipp, L T Perelman, I Itzkan, R R Dasari, M Feld *Phys. Rev. Lett.* **78** 1667 (1997)
232. H Xu, E J Bjerneld, M Kall, L Borjesson *Phys. Rev. Lett.* **83** 4357 (1999)
233. P Matějka, B Vlčková, J Vohlidal, P Pančoška, V Baumruk *J. Phys. Chem.* **96** 1361 (1992)
234. G Levi, J Pantigny, J P Marsault, D H Christensen, O Faurskov Nielsen, J Aubard *J. Phys. Chem.* **96** 926 (1992)
235. H I S Nogueira, P C R Soares-Santos, S M G Cruz, T Trindade *J. Mater. Chem.* **12** 2339 (2002)
236. S Yamamoto, K Fujiwara, H Watarai *Anal. Sci.* **20** 1347 (2004)
237. J R Lombardi, R L Birke, T Lu, J Xu *J. Chem. Phys.* **84** 4174 (1986)
238. G Bachelier, A Mlayah *Phys. Rev. B* **69** 205408 (2004)
239. O Stranik, R Nooney, C McDonagh, B D MacCraith *Plasmonics* **2** 15 (2007)
240. M Wu, J R Lakowicz, C D Geddes *J. Fluorescence* **15** 53 (2005)
241. J R Lakowicz, B P Maliwal, J Malicka, Z Gryczynski, I Gryczynski *J. Fluorescence* **12** 431 (2002)

242. I-Y S Lee, H Suzuki, K Ito, Y Yasuda *J. Phys. Chem. B* **108** 19368 (2004)
243. K Aslan, P Holley, C D Geddes *J. Mater. Chem.* **16** 2846 (2006)
244. M H Chowdhury, K Aslan, S N Malyn, J R Lakowicz, C D Geddes *J. Fluorescence* **16** 295 (2006)
245. K Aslan, Z Leonenko, J R Lakowicz, C D Geddes *J. Fluorescence* **15** 643 (2005)
246. A Yu Olenin, G V Romanovskaya, Yu A Krutyakov, G V Lisichkin, B K Zuev *Dokl. Akad. Nauk* **418** (2008) [e] (in the press)
247. C D Geddes, A Parfenov, I Gryczynski, J R Lakowicz *J. Phys. Chem. B* **107** 9989 (2003)
248. J R Lakowicz, I Gryczynski, J Malicka, Z Gryczynski, C D Geddes *J. Fluorescence* **12** 299 (2002)
249. K I Batarseh *J. Antimicrob. Chemother.* **54** 546 (2004)
250. M Yamanaka, K Hara, J Kudo *Appl. Environ. Microbiol.* **71** 7589 (2005)
251. I J Davis, H Richards, P Mullany *Oral Microbiol. Immunol.* **20** 191 (2005)
252. Y Matsumura, K Yoshikata, S Kunisaki, T Tsuchido *Appl. Environ. Microbiol.* **69** 4278 (2003)
253. L Balogh, D R Swanson, D Tomalia, G L Hagnauer, A T McManus *Nano Lett.* **1** 18 (2001)
254. A Melaiye, Z Sun, K Hindi, A Milsted, D Ely, D H Reneker, C A Tessier, W J Youngs *J. Am. Chem. Soc.* **127** 2285 (2005)
255. P Podsiadlo, S Paternel, J M Rouillard, Z Zhang, J Lee, J W Lee, E Gulari, N A Kotov *Langmuir* **21** 11915 (2005)
256. R W Sun, R Chen, N P Chung, C M Ho, C L Lin, C M Che *Chem. Commun.* 5059 (2005)
257. A J Bard, K B Holt *Biochemistry* **44** 13214 (2005)
258. S Silver *FEMS Microbiol. Rev.* **27** 341 (2003)
259. S Silver, L T Phung, G Silver *J. Ind. Microbiol. Biotechnol.* **33** 627 (2006)
260. J L Clement, P S Jarrett *Metal-Based Drugs* **1** 467 (1994)
261. G D Wright *Adv. Drug Deliv. Rev.* **57** 1451 (2005)
262. J R Morones, J L Elechiguerra, A Camacho, K Holt, J B Kouri, J T Ramirez, M J Yacaman *Nanotechnology* **16** 2346 (2005)
263. J G Allpress, J V Sanders *Surf. Sci.* **7** 1 (1967)
264. D W Hatchett, H S White *J. Phys. Chem.* **100** 9854 (1996)
265. P M Ajayan, L D Marks *Phys. Rev. Lett.* **60** 585 (1988)
266. I Sondi, B Salopek-Sondi *J. Colloid Interface Sci.* **275** 177 (2004)
267. J L Elechiguerra, J L Burt, J R Morones, A Camacho-Bragado, X Gao, H H Lara, M J Yacaman *J. Nanobiotechnol.* **3** : 6 1 (2005)
268. M J Forster, B Mulloy, M V Nermut *J. Mol. Biol.* **298** 841 (2000)
269. C K Leonard, M W Spellman, L Riddle, R J Harris, J N Thomas, T J Gregory *J. Biol. Chem.* **265** 10373 (1990)
270. H R Gelderblom, E H S Hausmann, M Ozel, G Pauli, M A Koch *Virology* **156** 171 (1987)
271. C-N Lok, C-M Ho, R Chen, Q-Y He, W-Y Yu, H Sun, P K-H Tam, J-F Chiu, C-M Che *J. Biol. Inorg. Chem.* **12** 527 (2007)
272. A Gupta, K Matsui, J F Lo, S Silver *Nat. Med. (N.Y.)* **5** 183 (1999)
273. X Z Li, H Nikaido, K E Williams *J. Bacteriol.* **179** 6127 (1997)
274. C Burda, X Chen, R Narayanan, M A El-Sayed *Chem. Rev.* **105** 1025 (2005)
275. S Pal, Y K Tak, J M Song *Appl. Environ. Micribiol.* **73** 1712 (2007)
276. A R Shahverdi, A Fakhimi, H R Shahverdi, S Minaian *Nanomedicine* **3** 168 (2007)
277. J Fu, J Ji, D Fan, J Shen *J. Biomed. Mater. Res., Part A* **79A** 665 (2006)
278. J-W Rhim, S-I Hong, H-M Park, P K W Ng *J. Agric. Food Chem.* **54** 5814 (2006)
279. H J Lee, S Y Yeo, S H Jeong *J. Mater. Sci.* **38** 2199 (2003)
280. W J Ye, M F Leung, J Xin, T L Kwong, D K L Lee, P Li *Polymer* **46** 10538 (2005)
281. S T Dubas, P Kumlangdudsana, P Potiyaraj *Colloids Surf., A* **289** 105 (2006)
282. H J Lee, S H Jeong *Textile Res. J.* **75** 551 (2005)
283. G Oberdörster, E Oberdörster, J Oberdörster *Environ. Health Perspect.* **113** 823 (2005)
284. G Oberdörster, V Stone, K Donaldson *Nanotoxicology* **1** 2 (2007)
285. A Nel, T Xia, L Mldler, N Li *Science* **311** 622 (2006)

[a] — *J. Anal. Chem. (Engl. Transl.)*
[b] — *Colloid. J. (Engl. Transl.)*
[c] — *Russ. J. Coord. Chem. (Engl. Transl.)*
[d] — *Russ. J. Phys. Chem. (Engl. Transl.)*
[e] — *Dokl. Chem. (Engl. Transl.)*